

Vibration–Rotation Molecular Constants for the Ground and ($\nu_3 = 1$) States of $^{32}\text{SF}_6$ from Saturated Absorption Spectroscopy

BERNARD BOBIN

*Laboratoire de Spectrométrie Moléculaire et Instrumentation Laser,¹
Université de Bourgogne, 6 Bld Gabriel, 21100 Dijon, France*

AND

CHRISTIAN J. BORDÉ, JACQUES BORDÉ, AND CHRISTIAN BRÉANT

*Laboratoire de Physique des Lasers,¹ Université de Paris-Nord,
Av. J.-B. Clément, 93430 Villetaneuse, France*

An analysis has been made of the vibration–rotation structure of the ν_3 band of $^{32}\text{SF}_6$ from measurements, by saturated absorption spectroscopy, of the frequencies for 136 transitions in close coincidence with CO_2 and N_2O laser lines in the 28-THz region. After deconvolution of the fine structure lines from their hyperfine structures, the centers of vibration–rotation transitions are given with a 5-kHz uncertainty. They are analyzed using the tensor Hamiltonian of Moret-Bailly, developed to the fifth order of approximation. An iterative procedure, using full diagonalization of the Hamiltonian matrices, leads to a very accurate determination of 18 effective molecular constants of the ($\nu_3 = 1$) excited state, together with 6 constants of the ground state (both for scalar and tensor terms). For instance, the inertial constant of the ground state is $\beta_0 = B_0 = 0.0910842001(10) \text{ cm}^{-1}$, the vibrational energy is $\alpha = \nu_3 = 948.10252337(40) \text{ cm}^{-1}$, and the Coriolis coupling coefficient is $\zeta_3 = 0.69344341(20)$. The recorded transitions, ranging from $P(84)$ to $R(94)$, are reproduced with a standard deviation $\sigma_d = 28 \text{ kHz} \simeq 0.93 \times 10^{-6} \text{ cm}^{-1}$. A few transitions remain out of the fit, and the possibility of resonances with close vibrational levels is briefly discussed. We also give the predicted positions for SF_6 transitions in close coincidence with laser lines of various isotopic species of CO_2 . © 1987 Academic Press, Inc.

I. INTRODUCTION

The advent of laser absolute frequency measurements has drastically changed the character of infrared molecular spectroscopy, first, through a qualitative shift from wavelength to frequency measurements, second, through a quantitative jump in accuracy across orders of magnitude; as a consequence, line frequency measurements are now performed in kilohertz instead of thousandths of cm^{-1} ($10^{-3} \text{ cm}^{-1} \simeq 30 \text{ MHz}$).

In a first step, sub-Doppler spectroscopic techniques have revealed many superfine, hyperfine, and superhyperfine features of tight clusters or of individual vibration–rotation lines. But another important question, which comes to mind next, is to find out whether such techniques can also bring a better global understanding of a full vibration–rotation band.

¹ Unités de Recherches Associées au CNRS.

Among all possible varieties of molecular spectra, one of the most extensively studied and well-known types of band is the ν_3 band of spherical tops (with the possible exception of the CO_2 laser bands themselves). One reason is of course the present interest stimulated by laser isotope separation, but even long before this motivation was put forward, the high symmetry of these molecules had attracted the attention of many group theorists.

Furthermore, since the advent of lasers, a remarkable series of coincidences between laser emission lines and absorption bands has favored the ν_3 bands of spherical tops: this has been the case for methane at $3.39 \mu\text{m}$. Also a remarkable match of frequencies has been found between CO_2 laser lines and the ν_3 bands of SF_6 , OsO_4 , and SiF_4 , to quote only a few.

At this point, the ν_3 band of SF_6 appears as a naturally good candidate for trying to answer the question raised above in the case of nonlinear polyatomic molecules, and the present paper is a first successful attempt to fit such a vibration-rotation band at the 30-kHz ($\sim 10^{-6} \text{ cm}^{-1}$) level.

In Section II, we present an historical survey of our frequency measurements, and show that a final common accuracy of 5 kHz may be retained (except when the N_2O laser is involved). Then a brief discussion of hyperfine interactions in spherical tops is given, in order to show how the centers of vibration-rotation lines can be derived from the various superfine, hyperfine, or superhyperfine structures. A complete calculation of line intensities is also presented.

In Section III, we develop the theoretical background for the present analysis, using the spherical tensor Hamiltonian introduced by J. Moret-Bailly in 1961. It may be surprising for the reader to find here again the description of this formalism, more than 20 years after its first publication. The reason is that, although this theory is now widely used by the specialists of spherical tops, it has not always been correctly or completely used. So, this section should be considered as a guide, where we give explicit formulae for the Hamiltonian matrix elements (in a triply degenerate vibrational state), and a short description of the analysis procedure, especially from the numerical point of view.

Finally, the analysis of ν_3 of SF_6 is presented in Section IV. Effective molecular constants for the ground and for the ($\nu_3 = 1$) states are tabulated. Computed and measured frequencies are compared for the 136 transitions which are involved in the analysis. A brief discussion suggests an explanation for the discrepancies which are observed for a few lines. A list of predicted close coincidences between lines of SF_6 and lines of other isotopic species of CO_2 is also published.

II. HISTORICAL DEVELOPMENT, PRESENTATION, AND ACCURACY OF THE MEASUREMENTS

The set of vibration-rotation frequencies used in this work has been obtained from spectroscopic structures recorded at different periods during the years 1976-1984, with the saturation spectrometer of Villetaneuse at various stages of its development. One will find a full presentation of this spectrometer and of its laser sources in Ref. (1). The CO_2 and N_2O laser lines which have been used in this series of measurements on the SF_6 molecule are shown on Fig. 1, together with a contour of the ν_3 -band region of SF_6 . The hyperfine structure of most of the recorded lines is now well resolved,

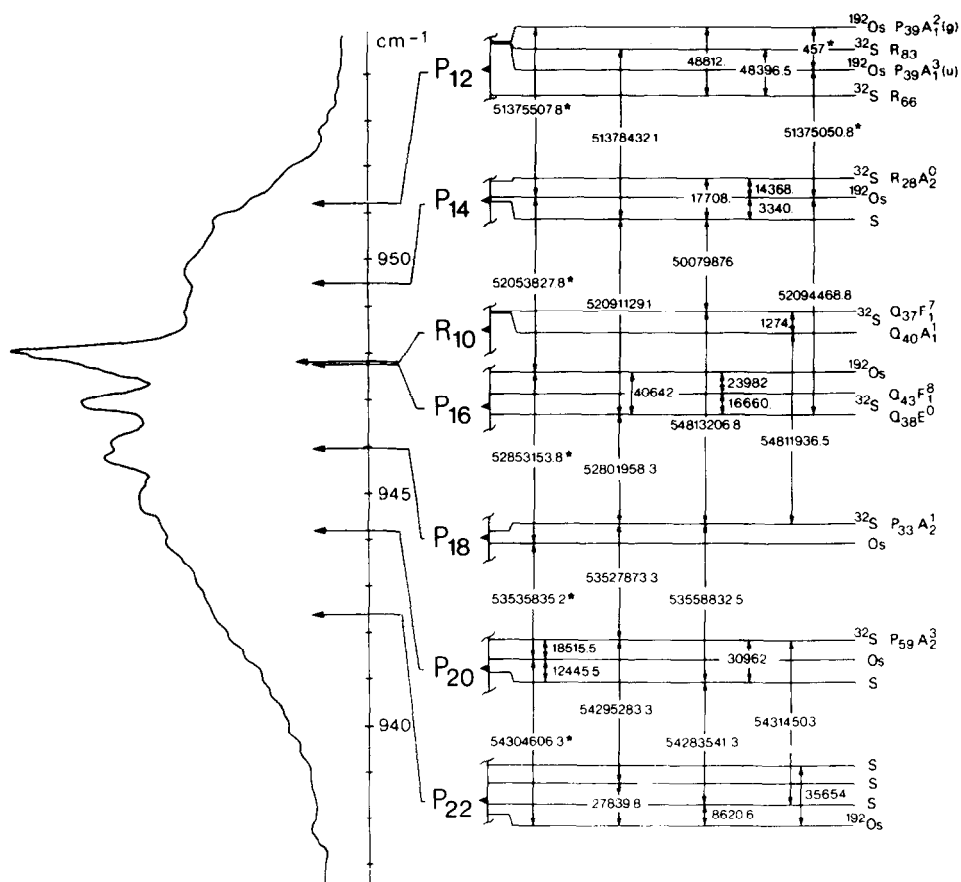


FIG. 1. The envelope of the ν_3 band of SF_6 , recorded on a Girard grid spectrometer by Brunet and Perez (2), is shown on the left part, while the right part of the figure displays the grid of CO_2 and N_2O (R10) laser lines which have been used in the present work to sample the band, together with a few of the frequency markers (17) used for the absolute frequency calibration of our saturation spectra.

with the exception of the lines recorded with the N_2O laser which were never studied again at the highest possible resolution.

The detailed study of this hyperfine structure was the primary motivation for the continued interest in pushing resolution and accuracy, but it appeared that the number of vibration-rotation lines which happened to be known after these years was large enough to become a significant test of the vibration-rotation Hamiltonian itself. These various vibration-rotation line frequencies have been determined with very different accuracies, depending on experimental techniques available at each period of time along these years of building the spectrometer, and, as we shall see, the set of data has therefore a great deal of inhomogeneity when used toward this new goal of determining vibration-rotation constants. Nevertheless, the overall experimental accuracy is, in the end, comparable or even slightly better than the standard deviation of the theoretical fit, which can be considered, perhaps, as the most comfortable situation (for a while!).

A presentation of all the presently available data, and associated accuracy, is given in Subsection II.A.

The combined superfine and hyperfine levels of structures (which eventually and ultimately collapse into superhyperfine structures (3, 4)) result in complicated patterns, all of which will be presented in a future atlas, together with the corresponding calculated spectra. In the present paper, we limit ourselves to the fine structure problem. This, somehow arbitrary, separation requires a deconvolution of every vibration-rotation line from its hyperfine structure, which provides a determination of the vibration-rotation transition frequencies in the limit of all hyperfine constants turned to zero. This deconvolution procedure is presented in Subsection II.B.

II.A. Chronological Evolution of Line Frequency Measurements in Saturated Absorption Spectroscopy around 10 μm

Around 1977, i.e., before the era of frequency-controlled waveguide lasers, three kinds of data were available:

(1) a small number of frequency-calibrated and well-resolved hyperfine or superfine structures, corresponding to the few lines that could be reached with conventional low-pressure CO_2 lasers, e.g., $P(33) A_2(1)$, $R(28) A_2(0)$, or $P(59) A_2(3)$ (5), or the $Q(38) F_2(0)-E(0)-F_1(0)$ superfine triplet (6, 7), all recorded with a 5-kHz HWHM (half-width at half-maximum);

(2) a much larger set of beat frequencies between two lasers locked to individual fine structure lines that could be reached with high-pressure waveguide CO_2 lasers, but without any detailed knowledge of the structures within these lines (linewidth of the order of 20 to 40 kHz);

(3) finally, a few oscilloscope pictures of expected tight superfine doublets (e.g., $R(29) F_1(2)-F_2(1)$ or $P(58) F_2(9)-F_1(8)$) exhibited more complicated structures which were barely resolved and not understood at that time, and from which only approximate line centers could be evaluated.

Spectroscopic landscapes, corresponding to each CO_2 laser line and where all these SF_6 lines are displayed, were also recorded at the same period by a simple frequency sweep of the free-running waveguide laser for $P(12)$ (1, 8), $P(14)$ (1, 8, 9), $P(16)$ (1, 10-12), $P(18)$ (7), and $P(20)$ (1).

From this first set of measurements, 94 absolute frequencies of vibration-rotation lines, which had been assigned from previous diode laser spectra (43, 45), were known with respect to CO_2 lines in 1977 (using saturated fluorescence in CO_2 (13-15)), and could be used for a first fit of the band, with only 12 spectroscopic parameters, and a standard deviation of the order of 300 kHz (7).

In 1979 the spectra corresponding to $P(22)$ of CO_2 (11) and $R(10)$ of the N_2O lasers (1, 16) were investigated, to reach, respectively, high- J lines of the P branch of SF_6 and the $P(3)$ manifold.

The next major step has been the elaboration of a new grid of absolute frequency markers in the beginning of 1980, which was based upon the very narrow OsO_4 resonances (17, 18), in order to replace the CO_2 and N_2O grid which was inaccurate at that time; thanks to these measurements, a 20-kHz correction was brought to the CO_2 reference lines of Ref. (14). A precise connection between these new OsO_4 markers

and SF_6 lines was also worked out at the same time, and provided one or several accurately known reference SF_6 lines, for each of the previously quoted SF_6 waveguide spectra (17) (however, these SF_6 lines have hyperfine structures and, depending on the symmetry of these structures, the line centers of the unresolved lines may have a few kilohertz absolute frequency uncertainty).

A second overall survey of the ν_3 band of SF_6 , using the frequency offset-locking technique with a phase-locked waveguide laser, was performed in January 1982. In this technique, a low-pressure laser is used as a reference laser and is locked to the third derivative of a saturated absorption peak in auxiliary absorption cells. The goal is to obtain, for this first laser, the best long-term frequency stability in addition to a good spectral purity (~ 10 Hz). Then, the broadband (600 MHz) waveguide laser is frequency controlled by phase locking the beat note of these two lasers to the tunable frequency produced by a generator. With this method, the hyperfine structure of 104 vibration-rotation lines was resolved with the $P(12)$ to $P(22)$ lines of CO_2 . The accuracy of frequency measurements was, this time, limited by the setting of the offset and by the symmetry of the reference lines, and also by nonlinearities of the frequency sweep across the structures, which was then achieved by a purely analogic method: the frequency generator of the phase-lock loop was swept by a low-frequency voltage ramp and the frequency deviations introduced in the frequency axis by this system could reach values of the order of 1 kHz over a given hyperfine structure. This problem was later solved by the use of a programmable R.F. synthesizer. Also, in 1983, the spectrometer was fully computerized, which means that not only the frequency control (synthesizer, frequency counters) but also the data averaging were driven by a computer (HP 9826 model), thus replacing the analogic recording of spectra on an X - Y plotter with a digital recording on disks, with a very accurate correspondence between channels and frequency detuning (the linearity of the frequency axis depending only upon the synthesizer stability, of the order of a few Hertz).

In 1984, 21 new hyperfine structures were added to the 104 previously recorded in 1982. The absolute frequency accuracy of these 1984 data was then only limited by that of the reference frequency. The reference laser frequency may first suffer from a lack of permanent control of the setting of the true center of the reference line. Drifts may occur owing to time-dependent electronic offsets (induced, for example, by room-temperature changes along the day) and also owing to a time-dependent signal baseline (induced, for example, by slow pressure changes in the absorption cell). With a 100- to 200-kHz peak-to-peak linewidth, small offsets or a slightly asymmetric shape of the error signal can easily result in a few kilohertz shift. Any slight misadjustment of the laser beam geometry for the reference laser may be the source of such an asymmetry. Also, for a number of measurements, a poor choice of reference line (any line with internal structure such as the SF_6 lines discussed above) has introduced an uncertainty on absolute frequencies of the same magnitude, i.e., of the order of 5 kHz.

Presently this reference problem is taken care of by sequential scanning of the measured line and of a reference line, using the same cell and the same measurement laser, and hence with the same laser beam geometry. In this way the reference laser frequency is eliminated, except for possible slow drifts during the measurement time (less than 10 Hz/min) which are tracked and corrected for by the computer. Finally, the reference line should be chosen, whenever possible, among the markers free of

structure. In this respect, the most recent progress achieved during 1984–1985 in the calibration of saturation spectra around $10\ \mu\text{m}$ was the high precision link established between the CO_2 and OsO_4 grids of frequency markers (4, 19). This connection was made possible thanks to the direct observation of supernarrow (2 kHz HWHM) saturated absorption resonances in low-pressure CO_2 (about 5×10^{-5} Torr) over both a long path length (108 m) and a long integration time (20 min), and is also a consequence of the long-term computer control of the laser frequency, including frequency drifts of the reference laser. The link was established with the $P(12)$ and $P(14)$ lines, of direct importance in the $\text{SF}_6\ \nu_3$ -band region, and also for the $R(10)$ line of CO_2 which has been measured with respect to an OsO_4 line whose absolute frequency is known with a 50-Hz accuracy (20). The immediate result is a high degree of confidence in the absolute frequency of our OsO_4 and CO_2 markers, at the kilohertz level. The long-term result is the clear possibility to calibrate saturation spectra at the subkilohertz level of accuracy, if one is willing to spend enough time on each line to be measured.

Indeed, the main remaining source of error will still be the lineshape symmetry (of narrow lines only), which has to be carefully checked by systematic studies of the dependence with the laser beam geometry, laser power, gas pressure, and modulation parameters (frequency and modulation index).

Since the measurements used in the present paper correspond to so many different steps in the quality of the spectrometer and to unequal choices of reference lines, we have to discuss case by case the final estimated uncertainty.

For the $P(12)$ CO_2 laser line, most measurements, both in 1982 and 1984, have used the low-frequency component $A_1(3)_u$ of the $P(39)$ superfine doublet of $^{192}\text{OsO}_4$ to lock the reference laser frequency. A comparison of 10 measurements which were performed both in 1982 and 1984 shows that the absolute frequency of measured lines may vary by as much as ± 3.1 kHz, owing quite likely to a different adjustment of the reference laser. To include these extreme cases we will adopt a conservative error margin of ± 5 kHz. The $R(83)$ and $R(94)$ clusters were measured only in 1982 with $R(66)$ of SF_6 as the reference; given the slightly asymmetric hyperfine structure of this line, an error limit of ± 5 kHz appears also as a reasonable estimate in these two cases.

For the $P(14)$ CO_2 laser line, six lines were accurately measured both in 1982 and 1984. The four lines for which the good OsO_4 reference line at 28 464 676 938.5 kHz was used are within 2 kHz in each case ($R(28)$ $F_2(1)$, $F_1(1)$, $E(1)$, and $F_2(2)$). In the case of the complicated $R(29)$ $F_1(2)$ – $F_2(1)$ superfine doublet (which is illustrated by Fig. 2), a different reference line was used in 1984 (the $R(28)$ $A_2(0)$ line of SF_6) and the corresponding frequencies are found, respectively, 1.4 and 4.0 kHz lower than in 1982. These discrepancies illustrate again uncontrolled shifts and drifts of the reference laser frequency which were not set for all measurements with the same accuracy. An error bar of ± 5 kHz should again apply to all cases.

In the case of the N_2O $R(10)$ laser line, two lines, $Q(40)$ $A_1(1)$ and $Q(37)$ $F_1(7)$, belong to the reference grid established in 1980, and are known to ± 6 kHz. Other line frequencies can be obtained through the beat measurements of 1979 with the reference laser locked to $Q(37)$ $F_1(7)$, and their absolute frequencies have an overall uncertainty better than ± 10 kHz, except for the $P(3)$ $A_2(0)$ and $F_2(0)$ lines which have a wider unresolved hyperfine structure and, thus, cannot be defined to better than ± 20 kHz. Finally, the $P(3)$ $F_1(0)$ frequency was never measured by beating two locked lasers

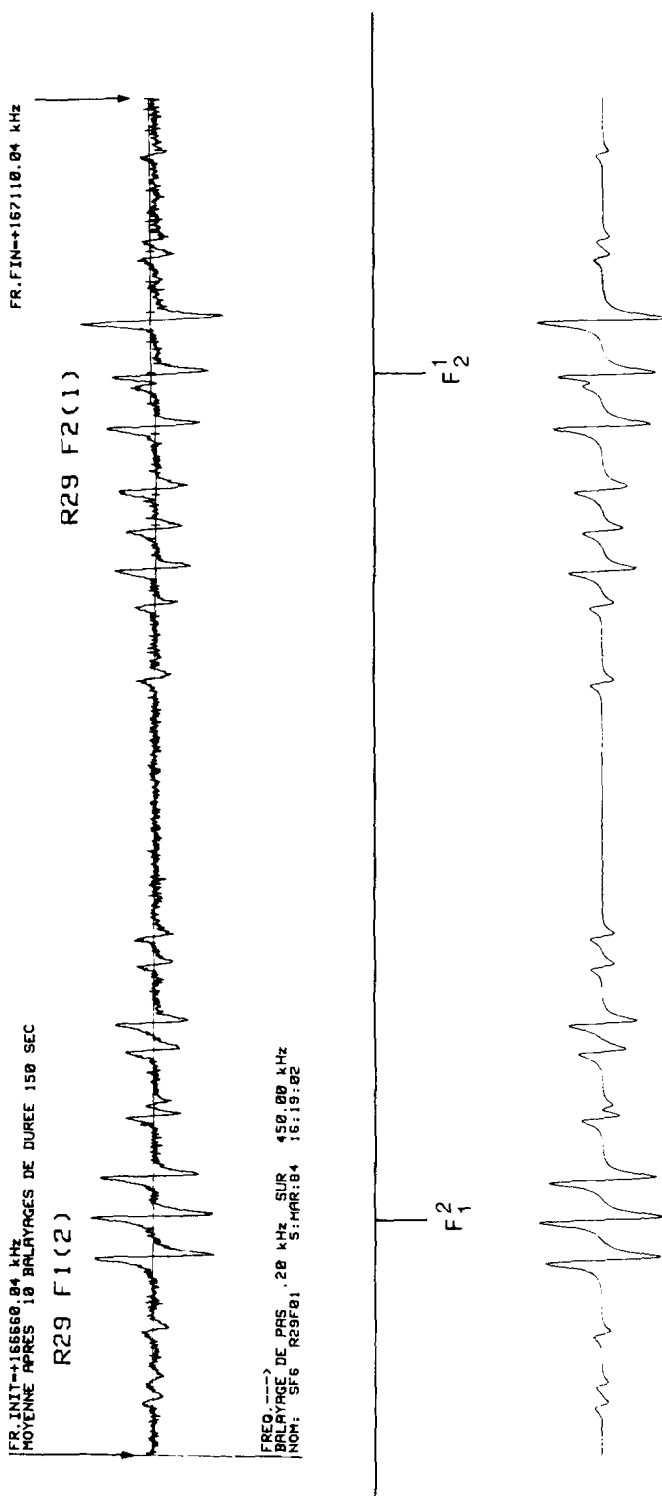


FIG. 2. Illustration of the deconvolution procedure in the case of a typical $F_1 - F_2$ tetragonal cluster, with its observed (top) and calculated (bottom) hyperfine structure. Besides the main $\Delta C = 0$ components, the spectrum exhibits many crossover resonances arising from the mixing of rovibrational states by hyperfine interactions (the evolution of such an $F_1 - F_2$ cluster from pure hyperfine to pure superhyperfine structures is illustrated by Fig. 4 of Ref. (4)). The parameters used to compute the structure in the present case are (in kHz) $I_{044} = 0.0057$, $I_{224} = 1125.58$, $c_a = -5.27$, $c'_a = c_a + \delta c_a = -5.279$, $A = 4.564$, $c_d = -4.6$, $c'_d = c_d + \delta c_d = -4.62$, and $X = -6.75$ (11, 12). The phenomenological correction for the rovibrational splitting was $\Delta E^{VR} = -10.2$ kHz (see text), and the HWHM of the Lorentzian lines is 1.75 kHz. The positions of the vibration-rotation line centers are indicated by the vertical bars, and the corresponding frequencies are obtained from the frequency distances of the lower and upper limits of the spectrum to the reference line, $R(28)4_2(0)$ of SF_6 in the present case.

together, but only by a fast reading of the line center frequency, and therefore cannot be claimed to be known to better than ± 50 kHz. The Q line frequencies had also been estimated in 1979, with a ± 15 -kHz accuracy, by a direct comparison with the N_2O line center (at 17.725 ± 0.010 MHz from $Q(37) F_1(7)$), to which the reference laser had been locked using the saturated fluorescence technique.

For $P(16)$ of CO_2 , the reference for 1982 and 1984 measurements has been the narrow and isolated SF_6 $Q(43) F_1(8)$ line whose absolute frequency measured against OsO_4 has been found to be $28\,412\,599\,128.7 \pm 2.0$ kHz (at $-23\,982 \pm 1$ kHz from the OsO_4 line and $+16\,660 \pm 2$ kHz from $Q(38) E(0)$ of SF_6). Twenty-one measurements common to 1982 and 1984, among the total number of 39, show an internal consistency of ± 2 kHz.

On the $P(18)$ CO_2 line, the reference laser was locked to $P(33) A_2(1)$ of SF_6 for the 1982 set of measurements, whereas a PF_5 line was used in 1984. If the 1984 measurements are converted in frequency differences with $P(33) A_2(1)$, they are all within 2 kHz of the 1982 line center determinations. Then, using the reference laser locked to the PF_5 line, the difference frequency between the center of the $P(33) A_2(1)$ line and the OsO_4 line was measured to be $10\,559.9$ kHz at high resolution, a result 6.5 kHz higher than the 1980 measurement. This difference can be easily understood in view of the expected asymmetry of the SF_6 line when its hyperfine structure is unresolved.

For $P(20)$ of CO_2 , 9 measurements out of the 16 performed in 1982 were reproduced in 1984 within 3 kHz, but the reference line in both cases was the $P(59) A_2(3)$ SF_6 line, which has a nontotally symmetric hyperfine structure. Since this line was unresolved when compared with the OsO_4 reference in 1980, our absolute frequencies may have an additional error of 2 or 3 kHz in this case.

For $P(22)$ of CO_2 , the beat frequency measurements performed in 1979 used the SF_6 line about 15.69 MHz above CO_2 as a reference. It was later discovered that this line has a complicated asymmetric structure. The 1982 and 1984 measurements of the 11 identified lines of SF_6 used a much more symmetric triplet (24 kHz wide) located 7813 ± 3 kHz above the previous reference (i.e., about 23.5 MHz above CO_2). By direct comparison of the central component of this triplet with the OsO_4 reference line, an absolute frequency equal to $28\,251\,965\,170 \pm 3$ kHz has been attributed to this new SF_6 reference. All 1984 measurements are within 3.5 kHz below the 1982 ones (and fully consistent with 1979 beat frequency measurements and the above change of reference line).

As a general conclusion, it appears that, using the best of 1982 and 1984 spectra, and except for lines measured with the N_2O laser, an upper common bound for the error bar equal to ± 5 kHz can be associated with all our measured frequencies (including the error introduced by the deconvolution procedure discussed below in Subsection II.B.3).

II.B. The Hyperfine Problem and the Deconvolution of Fine Structures

1. *Background on the hyperfine Hamiltonian and the corresponding structures.* Ideally, the analysis of the spectrum should be made with a simultaneous adjustment of rovibrational and hyperfine parameters. Practically one must start with a two-step analysis and disconnect first, as much as possible, the rovibrational problem from the

hyperfine interactions. Assuming that a reliable rovibrational assignment of a lower resolution spectrum has been worked out before, the first step is to reproduce individually the hyperfine patterns of each cluster of rovibrational lines. This step leads to a set of hyperfine coupling constants, with their dependence on the rovibrational states. This procedure has either confirmed the previous assignments, or given new assignments when the hyperfine structures had not been resolved before.

Basically the calculation of these structures has followed the procedure described in Refs. (11, 12), and, here, we shall only recall the main facts relevant to the present paper, and mention the improvements needed by the better resolution and the availability of an increased number of data.

(i) As it is well understood now, rovibrational levels, and hence lines, generally appear as clusters (see, for instance, Harter (3) and references therein, especially Dorney and Watson (58)); the energy splittings within a cluster, called the superfine splittings, can be extremely small, especially for high values of the quantum number R and toward the ends of each R manifold. Because the hyperfine operators may have nonzero matrix elements between different rovibrational states, one must treat simultaneously those states, which are close enough to be substantially mixed. Thus, the Hamiltonian matrix must include both rovibrational terms, which give the superfine splittings, and the hyperfine terms.

Because the splittings between clusters are much larger than those within a cluster, it is usually sufficient to set the matrix in the basis associated with a unique rovibrational cluster; however, in some cases we have extended the basis to include additional neighbor states, or adjacent full clusters. The states of the basis which are obtained by coupling rovibrational and nuclear spin states, are noted:

$$|(J, I)FM_F; (J, l)R, nC; v_3\rangle$$

where C denotes the octahedral symmetry species of the rovibrational state and n distinguishes states with identical R and C . The smallest bases are associated with the simplest $F_1 - F_2$ clusters and contain 12 hyperfine substates; the largest bases we have dealt with contain around 12 different rovibrational states (different (C, n)), leading to Hamiltonian matrices of dimension around 50. The clustering of levels is very similar in both vibrational states (ground and excited), except for a large scaling factor and, in fact, in most cases the mixing of different rovibrational states is important in the ground state only and not at all in the excited state. At increasing resolutions, the spectrum will then display first the superfine splittings (of the $(v_3 = 1)$ state essentially), then the hyperfine structures of each superfine component; but one must remember that these hyperfine structures will often be strongly perturbed by the ground state mixing. As mentioned before, for high- R values and toward the ends of R manifolds, the mixing can also be strong in the $(v_3 = 1)$ state (it is then even stronger in $(v_3 = 0)$), and we have all kinds of situations, up to the extreme one where the superfine splittings are negligible in both vibrational states, which leads to what is called a superhyperfine structure.

The rovibrational terms² that we introduce in the matrix in order to calculate the superfine splittings are:

² In this part of the present work the tensorial notations of Hecht have been used. T_{044} and T_{224} denote the main fourth-rank rovibrational tensors. The corresponding constants are related to those of Moret-Bailly (used in Sect. III) by: $t_{044} = 2(7/3)^{1/2}\epsilon$ and $t_{224} = -(7/3)^{1/2}\varphi$.

(1) the tensor centrifugal distortion operator T_{044} , with a constant t_{044} which was originally deduced from hyperfine structures (7, 21), and which splits both the ground and excited vibrational states;

(2) the tensor operator T_{224} , which has nonvanishing matrix elements only for $v_3 \neq 0$, and with a constant t_{224} deduced from previous rovibrational fits (7) (this constant is much greater than t_{044} , hence the scaling factor).

The matrix elements of these terms can be noted $E_T^{VR}(t_{044}, t_{224}, v_3, RnC)$.

In the ($v_3 = 1$) state, we also add phenomenological diagonal terms to take into account the effects of higher order corrections (such as those due to matrix elements off-diagonal in R), and which are necessary to adjust the computed superfine splittings. We note their contribution $\Delta E^{VR}(RnC)$.

Thus the rovibrational part of our Hamiltonian matrix is a simple diagonal matrix, made of

$$E_T^{VR}(t_{044}, t_{224}, v_3 = 1, RnC) + \Delta E^{VR}(RnC)$$

for the excited ($v_3 = 1$) vibrational state, and of

$$E_T^{VR}(t_{044}, v_3 = 0, RnC)$$

for the ground vibrational state ($v_3 = 0$).

To obtain the absolute frequencies, one should of course add scalar terms to the eigenvalues; their total contribution $E_{Sc}^{VR}(v_3)$ has no effect on the shape of the hyperfine structures, but merely shifts the whole structure.

(ii) To these rovibrational terms, we add the matrix elements of the hyperfine operators. The operators that were necessary to reproduce correctly the spectra are the scalar and tensor spin-rotation and spin-vibration, and the tensor spin-spin interaction terms. In addition we have introduced three higher order operators which express the dependence of the spin-rotation interaction with vibration.³

At this stage, we are able not only to calculate a frequency for any transition between respective hyperfine sublevels of two rovibrational clusters, but also to define "rovibrational" frequencies. These values are simply obtained by turning to zero all hyperfine coupling constants. In our case, since our rovibrational matrix is diagonal, the "rovibrational" frequencies are expressed as

$$[E_{Sc}^{VR}(v_3 = 1) - E_{Sc}^{VR}(v_3 = 0)] + [E_T^{VR}(t_{044}, t_{224}, v_3 = 1, RnC) + \Delta E^{VR}(RnC) - E_T^{VR}(t_{044}, v_3 = 0, RnC)]. \quad (1)$$

The tensor part (second bracket) gives the position of the "rovibrational" transitions (RnC) of a cluster, relatively to the hyperfine structure. Figure 2 shows an example of such a structure, with the computed spectrum (as described in Subsect. II.B.3); the vertical bars indicate the positions of the "rovibrational" frequencies. The corresponding absolute frequencies, which we use as data in the present paper, are deduced from the positions of these bars, with respect to the absolute frequency calibration of the experimental recording.

2. *Background on the intensity theory in saturation spectroscopy and application to the v_3 band of SF_6 .* The fit of the hyperfine structures and the deconvolution procedure

³ These three operators belong to a wider class of operators suggested by Michelot in her general theory of higher order hyperfine effects in spherical tops (33).

imply a detailed theoretical knowledge of the intensities of individual hyperfine components in saturation spectroscopy. Such a theory is still familiar only to experts in this specific spectroscopic technique, and we feel that, at this point, a short review of the main results of this intensity theory could be useful to the reader interested in the connection with ordinary linear spectroscopy of fine structure spectra of spherical tops. Indeed, in the limit of unresolved hyperfine structures, this theory gives an essential insight into the relationship between usual selection rules and statistical weights, and the true hyperfine content of rovibrational lines (including parity labels), and it illustrates a general principle of spectroscopic stability in nonlinear spectroscopy.

In linear spectroscopy, as illustrated by Fig. 3a, the absorption coefficient k is simply given by a summation over M sublevels of a second-order density matrix diagram (22):

$$k = \frac{1}{4\pi\epsilon_0} \frac{8\pi^3\nu}{hc} \frac{n_a}{g_a} \sum_{M_a, M_b} \langle bF_b M_b | \vec{\mu} \cdot \hat{\mathbf{e}}^* | aF_a M_a \rangle \times \langle aF_a M_a | \vec{\mu} \cdot \hat{\mathbf{e}} | bF_b M_b \rangle f(\nu - \nu_0) \quad (2)$$

where f is a normalized lineshape (e.g., $(1/\sqrt{\pi}\Delta\nu_D)\exp[-(\nu - \nu_0)^2/\Delta\nu_D^2]$ in the Doppler limit), $\vec{\mu}$ is the electric dipole moment operator, $\hat{\mathbf{e}}$ is the polarization unit vector of the electric field, and (n_a/g_a) is the population of each M sublevel of the lower state $|aF_a\rangle$.

The application of the Wigner-Eckart theorem is then followed by the evaluation of the sum of squared 3 - j symbols, which gives the familiar one-third factor:

$$\begin{aligned} \sum_{M_a, M_b} \langle bF_b M_b | \vec{\mu} \cdot \hat{\mathbf{e}}^* | aF_a M_a \rangle \langle aF_a M_a | \vec{\mu} \cdot \hat{\mathbf{e}} | bF_b M_b \rangle &= \sum_{M_a, M_b} |\langle bF_b M_b | \vec{\mu} \cdot \hat{\mathbf{e}}^* | aF_a M_a \rangle|^2 \\ &= |\langle bF_b || \mu^{(1)} || aF_a \rangle|^2 \sum_{M_a, M_b} \begin{pmatrix} F_b & 1 & F_a \\ -M_b & q & M_a \end{pmatrix}^2 = \frac{1}{3} |\langle bF_b || \mu^{(1)} || aF_a \rangle|^2. \end{aligned} \quad (3)$$

Finally, the absorption coefficient is

$$k = \frac{4\pi^2}{3} \alpha \frac{n_a}{g_a} \nu f(\nu - \nu_0) [|\langle bF_b || \mu^{(1)} || aF_a \rangle|^2 / e^2] \quad (4)$$

where a cross section has been displayed together with the introduction of the fine structure constant α .

For the evaluation of the population⁴ in the case of SF_6 , we have

$$\frac{n_a}{g_a} = \frac{N}{Z_V Z_R} \exp(-E_a/k_B T) \quad (5)$$

(see, for example, Appendix II of Ref. (1)).

The reduced matrix element can be calculated using the double Racah algebra, associated with Judd's double tensors formalism and the chain of groups $^{(L)}O(3) \times ^{(M)}O(3) \supset ^{(L)}O(3) \times O_h$ (23). With the notations of Ref. (11) for the hyperfine state

⁴ In this formula, Z_V and Z_R are, respectively, the vibrational and rotational partition functions (taking spin degeneracy and the Pauli principle into account): $Z_V = \prod_{i=1,6} [1 - \exp(-h\nu_i/k_B T)]^{-d_i}$, where d_i is the degeneracy of the vibrational mode ν_i ; and $Z_R \approx (8\pi^{1/2}/3)\alpha_T^{3/2} \exp(\alpha_T/4)$ with $\alpha_T = B_0 hc/k_B T$. The Boltzmann factor of the lower state is $\exp(-E_a/k_B T) = \exp[-\alpha_T J(J+1)]$, and we have $N = 3.2958 \times 10^{22}$ molecules/ m^3 for 1 Torr of perfect gas, at the temperature of 293 K.

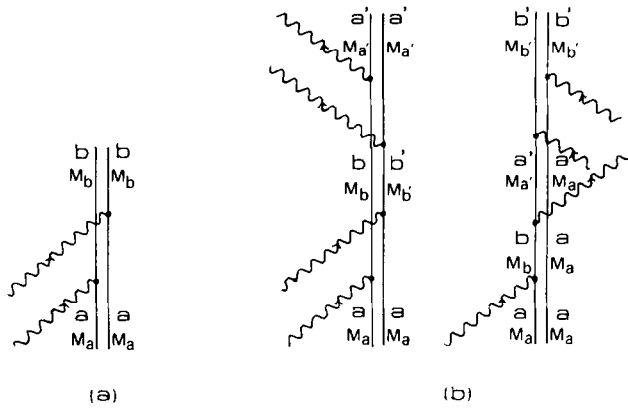


FIG. 3. Density matrix diagrams (22) corresponding to (a) linear absorption and (b) saturated absorption. These diagrams have complex conjugate analogs. There are also corresponding diagrams starting with the upper state population, which contribute proportionally to n_b/g_b with a negative sign, and which have been neglected for the sake of simplicity in the present paper.

vectors and those of Griffith (57) for \mathbf{V} and \mathbf{X} symbols, we can write the Wigner-Eckart theorem for the electric dipole moment as

$$\begin{aligned}
 & \langle (J_\tau I_g) F_\tau M_F; ((J_\tau l_\rho) R_\lambda n' C_R C_S) A_{2u}; v_3, \alpha | \mu_q^{(1_u, 0_g, A_{1g})} (J'_{\tau'} I'_g) F'_{\tau'} M'_{F'}; \\
 & ((J'_{\tau'} l'_{\rho'}) R'_{\lambda'} n' C'_R C'_S) A_{2u}; v'_3, \alpha' \rangle = (-1)^{F-M_F} \begin{pmatrix} F_\tau & 1_u & F'_{\tau'} \\ -M_F & q & M'_{F'} \end{pmatrix} \mathbf{V} \begin{pmatrix} A_{2u} & A_{1g} & A_{2u} \\ \iota & \iota & \iota \end{pmatrix} \\
 & \times [3(2F+1)(2F'+1)]^{1/2} \cdot ([A_{1g}][A_{2u}][A_{2u}])^{1/2} \begin{Bmatrix} J'_{\tau'} & I'_g & F'_{\tau'} \\ 1_u & 0_g & 1_u \\ J_\tau & I_g & F_\tau \end{Bmatrix} \mathbf{X} \begin{bmatrix} A_{1g} & A_{1g} & A_{1g} \\ C'_R & C'_S & A_{2u} \\ C_R & C_S & A_{2u} \end{bmatrix} \\
 & \times [(C_S)(2I+1)]^{1/2} \delta_{II'} \delta_{C_S C'_S} (-1)^{R} \mathbf{K}_{(n C_R A_{1g} n' C'_R)}^{(R_\lambda 0_g R'_{\lambda'})} [(2R+1)(2R'+1)]^{1/2} \\
 & \times \begin{Bmatrix} J'_{\tau'} & l'_{\rho'} & R'_{\lambda'} \\ 1_u & 1_u & 0_g \\ J_\tau & l_\rho & R_\lambda \end{Bmatrix} \langle J_\tau J_\tau \| \mathbf{D}^{(1_u, 1_u)} \| J'_{\tau'} J'_{\tau'} \rangle \cdot \langle 0_g; l_\rho; v_3 \| \mathbf{q}_3^{(0_g, 1_u)} \| 0_g; l'_{\rho'}; v'_3 \rangle \mu_3 \delta_{\alpha\alpha'} \quad (6)
 \end{aligned}$$

where the dipole moment operator in the rotating frame has been reduced to the first term of its expansion in dimensionless normal coordinates⁵:

$$\mu^{(0_g, 1_u)} = \mu_3 \mathbf{q}_3^{(0_g, 1_u)} \quad \text{with} \quad \mu_3 = \frac{\partial \mu_\alpha}{\partial q_{3\alpha}} \quad (7)$$

The expression of the isoscalar coefficient is

$$\mathbf{K}_{(n C_R A_{1g} n' C'_R)}^{(R_\lambda 0_g R'_{\lambda'})} = (-1)^R \delta_{RR'} \delta_{nn'} \delta_{C_R C'_R} \delta_{\lambda\lambda'} ([C_R]/(2R+1))^{1/2} \quad (8)$$

⁵ In their study of ν_4 of SF₆, Person and Krohn (24) found that an additional term was needed to correctly reproduce the intensities of the observed lines. Such a term may also be introduced for ν_3 . In fact, this is only a particular application of the general expansion of the dipole moment operator. For spherical tops, a general development in tensor form (similar to that of the Hamiltonian) was first introduced by Pascaud (25), and then generalized and successfully applied to several problems by Loëte (26).

and the reduced matrix elements of $\mathbf{D}^{(1_u, 1_u)}$ and $\mathbf{q}_3^{(0_g, 1_u)}$ are, respectively, given by

$$\langle J_\tau J_\tau \| \mathbf{D}^{(1_u, 1_u)} \| J'_\tau J'_\tau \rangle = (-1)^{1+J-J'} [3(2J+1)(2J'+1)]^{1/2} \delta_{\tau, \tau' \times u} \quad (9)$$

$$\langle 0_g; l_\rho = 0_g; v_3 = 0 \| \mathbf{q}_3^{(0_g, 1_u)} \| 0_g; l'_\rho = 1_u; v'_3 = 1 \rangle = -(3/2)^{1/2} \quad (10)$$

so that μ_3 is related to the vibrational transition moment μ_{01} introduced by Fox (27) and Fox and Person (28) by

$$\mu_3 = \sqrt{2} \mu_{01} \quad (11)$$

with $\mu_{01} = 0.437 \pm 0.005$ D, according to Ref. (29) (1 D = 10^{-18} esu. cm = 0.333564×10^{-29} C.m).

The final result for the dipole moment matrix element is therefore (without expliciting all the quantum numbers which are to be taken from Eq. (6))

$$\begin{aligned} & \langle (\text{q.n.}) | \mu_q^{(1_u, 0_g A_1 g)} | (\text{q.n.})' \rangle \\ &= (-1)^{F-M_F} \begin{pmatrix} F_\tau & 1_u & F'_{\tau'} \\ -M_F & q & M'_{F'} \end{pmatrix} \times [(2F+1)(2F'+1)]^{1/2} \begin{Bmatrix} J & F' & I \\ F & J & 1 \end{Bmatrix} \frac{\mu_3}{\sqrt{2}} \\ & \times (2J'+1)^{1/2} \times (-1)^{F'+I+J'+1} \times \delta_{II'} \delta_{C_R C'_R} \delta_{C_S C'_S} \delta(A_{2u}, C_R, C_S) \delta_{RR'} \delta_{JR} \delta_{I'1} \delta_{nm'} \delta_{\lambda\lambda'} \quad (12) \end{aligned}$$

where all the selection rules appear explicitly as δ symbols.

If any of the quantum numbers (q.n.) loses its significance to label eigenstates of the Hamiltonian (because of mixing through any off-diagonal interaction, e.g., the hyperfine Hamiltonian), new reduced matrix elements will be obtained with the coefficients α'^* and α'' of the transformation matrices corresponding, respectively, to the upper and lower energy eigenstates:

$$\begin{aligned} \langle i \| \mu^{(1)} \| j \rangle &= \sum_{C, I, \dots} \alpha_{i, CI, \dots}^{(F, v_3=1)*} \alpha_{j, CI, \dots}^{(F, v_3=0)} \\ & \times \langle (JI)F'; J'I'RC_R C_S \dots; v_3 = 1 \| \mu^{(1_u, 0_g A_1 g)} \| (JI)F; JI \dots; v_3 = 0 \rangle. \quad (13) \end{aligned}$$

If the $[\alpha]$ matrices are almost identical in both states and if the reduced matrix elements have no or little dependence with C, I, \dots (e.g., for superhyperfine structures), then, owing to the orthogonality of the coefficients, new selection rules δ_{ij} will result from the selection rules $\delta_{C_R C'_R} \delta_{I' \dots}$ before diagonalization.

In the low field limit of saturation spectroscopy (which corresponds to the experimental situation for ultrahigh resolution), observed signals are described by fourth-order density matrix diagrams (four-wave mixing), as shown on Fig. 3b. This means that any such process requires a quadruple product of matrix elements of the electric dipole moment operator, and hence four successive applications of the Wigner-Eckart theorem, followed by a summation over all M sublevel possibilities. The corresponding calculation can be found in Ref. (30) for each type of resonance (main two-level recoil peaks, crossover resonances, hyperfine coherence-induced saturation resonances). The sums of products of 3 - j symbols are given by

$$\begin{aligned} A_{\alpha\beta\beta'\alpha'} &= (-1)^{F_{\alpha'}+F_{\alpha'}} \sum_{k=0,1,2} (-1)^{q^-+q^+} (2k+1) \begin{pmatrix} k & 1 & 1 \\ 0 & -q^- & q^- \end{pmatrix} \begin{pmatrix} k & 1 & 1 \\ 0 & -q^+ & q^+ \end{pmatrix} \\ & \times \left\{ \begin{matrix} k & 1 & 1 \\ F_\alpha & F_\beta & F_{\beta'} \end{matrix} \right\} \left\{ \begin{matrix} k & 1 & 1 \\ F_{\alpha'} & F_\beta & F_{\beta'} \end{matrix} \right\} \quad (14) \end{aligned}$$

where $(\alpha\beta\beta'\alpha') = (abb'a')$ or $(baa'b')$, according to the notations of Fig. 3. This result is also a direct application of the Wigner-Eckart theorem in Liouville space (22). With the usual configuration of our spectrometer, we have $q^+ \equiv q^- = 1$ (retroreflected circularly polarized light).

As an example, these angular factors A are given by the following expressions for the main recoil peaks:

$$A_{abba} \equiv A_{baab} = \begin{cases} \frac{12F^2 - 2}{15(2F - 1)2F(2F + 1)} & \text{for } \Delta F = \pm 1 \\ \frac{2F(F + 1) + 1}{15(2F + 1)F(F + 1)} & \text{for } \Delta F = 0 \end{cases} \quad (15)$$

with $F = \sup(F_a, F_b)$. For crossover resonances similar formulae will be found in Ref. (30).

Besides this A factor, the intensity of each line will be proportional also to the level population (n_a/g_a), as in the linear absorption case, and, this time, to the product of four (instead of two) reduced matrix elements corresponding to the relevant diagram.

It is to be noted that, in the limit of vanishing hyperfine structures, and for a given value of I , the sum over all hyperfine intensities results in a formula identical to Eq. (14) but with J replacing F , and with the nuclear spin degeneracy $(2I + 1)$ as a multiplicative factor, as demonstrated in Ref. (30). Then, for a given vibration-rotation line, the sum over possible values of I runs only over the values allowed by the Pauli principle $\delta(A_{2u}, C_R, C_S)$, and leads to the following statistical weights (31, 32) $g_S(C_R) = \sum_I (2I + 1)$:

symmetry C_R :	A_{1g}	A_{1u}	A_{2g}	A_{2u}	E_g	E_u	F_{1g}	F_{1u}	F_{2g}	F_{2u}
values of I :	0	0	—	1, 3	—	1, 2	1	1	0, 2	—
weight $g_S(C_R)$:	1	1	0	10	0	8	3	3	6	0

Note that our present results are consistent with those of Cantrell and Galbraith (59), but that we use a different theoretical approach.

In this limit, the intensity of a vibration-rotation line defined by the transition ($J_a \rightarrow J_b, C$) is proportional to

$$\frac{N}{Z_R Z_V} e^{-\alpha T J_a(J_a+1)} g_S(C) [A_{abba}(J) + A_{baab}(J)] | \langle bJ_b || \mu || aJ_a \rangle |^4 \quad (16)$$

where $J = \sup(J_a, J_b)$ and with

$$| \langle bJ_b || \mu || aJ_a \rangle |^4 = (2J_b + 1)^2 \mu_{01}^4. \quad (17)$$

For our spectra, the relative intensities of distant vibration-rotation lines are usually only indicative, since the laser intensity, which also comes as a multiplicative factor, is not kept to a constant level throughout the laser output profile, and drops down quickly near the mode profile edges.

3. *Synthetic spectra and derivation of vibration-rotation frequencies.* Once we have the frequencies and intensities of all transitions between hyperfine substates, as described in the preceding subsections, we can draw synthetic spectra on a computer plotter, through a convolution with a Lorentzian lineshape (see Fig. 2 as an example).

The width of the lineshape is adjusted for each recording. Once a synthetic spectrum is drawn and satisfactorily reproduces the observed spectrum, one can retrieve the absolute frequencies of all transitions from the absolute frequency measurement of the observed contour, and, in particular, the vibration-rotation frequencies (which are marked with vertical bars as on Fig. 2).

To do so, we superimpose the observed and calculated contours, both drawn at the same scale. Given a digitally recorded contour, one could think of a better procedure than a mere superposition of two drawings; however, it has not yet been possible to do better for the present set of data since:

- (i) the 1982 recordings were not in digital form,
- (ii) the 1984 spectra are digitalized on a HP desk-top computer which is not linked with the CDC computer of theoretical contours,
- (iii) the number of hyperfine components (main lines and crossovers) contributing to each observed feature is far too large (up to 120 in our study) to ensure a unique least-squares solution; however, for some specific structures with well-isolated lines, we have succeeded in using such a least-squares procedure both to reproduce the spectrum and to retrieve the hyperfine constants.

This rather cumbersome procedure of superimposition certainly increases the uncertainty of the final vibration-rotation data, by introducing additive sources of errors:

- (i) superimposing the two contours and measuring the position of the bars marking the frequencies are limited, anyway, by the thickness of the pencil line;
- (ii) the fit of the hyperfine structure is not always perfect, which leads to some additional freedom;
- (iii) the rovibrational terms included in the Hamiltonian are limited to the fourth order in our model, and work as effective terms. Using a more sophisticated rovibrational Hamiltonian (such as the one described in the next section) can change slightly the hyperfine parameters, which, in turn, will slightly change the positions of the derived rovibrational data. So we should consider that we have only done the first round of an iterative procedure.

We can, however, estimate that the errors due to these considerations do not exceed 1 kHz, which is small considering the fact that without a deconvolution it would have been impossible to locate the rovibrational line centers to better than 20 kHz. A particularly striking example is the $Q(52) A_1(2)$ line, whose two components A_{1g} and A_{1u} show a splitting of 30 kHz: only a precise study of the hyperfine structure enables us to say that the rovibrational transition should be located exactly on top of the A_{1g} component!

III. THE VIBRATION-ROTATION HAMILTONIAN AND THE NUMERICAL ANALYSIS

In the case of triply degenerate vibrational levels of spherical tops (in their ground electronic state), the Hamiltonian developed by Moret-Bailly (34) is now recognized as an especially powerful tool, and has been widely used with great success during the last 20 years. We shall not give here a complete demonstration of its general features, but we think it may be useful to recall the bases of the theory, to give adequate formulae for the present problem, and to briefly describe the numerical procedure which is used to analyze such a vibrational band.

First, let us specify that what we are going to write is adapted to A_1 - and F_2 -type

vibrational levels of XY_4 molecules, the symmetry group of which is T_d , but that most results are immediately applicable to A_{1g} and F_{1u} levels of XY_6 octahedral molecules (symmetry group O_h), as we shall explain at the end of Section III.B.

III.A. The Tensor Vibration-Rotation Hamiltonian in $O(3)$

Using group theory and irreducible tensors algebra, Moret-Bailly (34) has shown that it was possible to write an a priori Hamiltonian operator for spherical tops with irreducible tensors of the full rotation group $O(3)$, except when the $\nu_2(E)$ vibrational mode is excited (this restriction was later removed by Michelot (35)). This Hamiltonian is then a linear combination of tensors of $O(3)$:

$$\mathbf{H} = \sum_k {}^k \mathbf{O}_{A_1}^{(n)} \quad (18)$$

where ${}^k \mathbf{O}_{A_1}^{(n)}$ results from the coupling between a rotational tensor (related to the rigid rotator) and vibrational ones (related to the four normal modes of XY_4 tetrahedral molecules). Since \mathbf{H} must be invariant in any operation of the T_d group, that is must be of symmetry A_1 , the total tensorial rank n may take the values

$$n = 0_g, 4_g, 6_g, 8_g, \dots$$

as shown by the reduction in T_d of the representation $D^{(n_g)}$ of $O(3)$. Each rotational or vibrational term itself results from the coupling of several elementary operators.

Basis functions are also built in tensor form, using a similar procedure, and the same coupling scheme. The great advantage of this formalism is that the Hamiltonian is, by construction, diagonal with respect to the vibrational quantum numbers v_s , the total angular quantum number J , and a symmetry label C , which represents one of the five irreducible representations of T_d (A_1, A_2, E, F_1 , and F_2). Then, for a given vibrational level (given v_s), and a given J , the Hamiltonian matrix is reduced in block-diagonal form (each block is specified by the label C), and the diagonalization then takes place in these blocks of rather small dimension (for instance the largest matrix we dealt with in the present analysis was of dimension 75×75 , for $J = 95$ and $C = F_2$).

The calculation of the matrix elements of \mathbf{H} requires the introduction of $3n - j$ recoupling symbols and, via the Wigner-Eckart theorem, of the \mathbf{F} symbols adapted to the cubic symmetry (and known as Moret-Bailly's \mathbf{F} symbols).

After diagonalization (and in the limit where the mixing of states is not important), each eigenvalue, that is each rovibrational level, is then labeled by four quantum numbers (in addition to the vibrational ones):

- (1) the total angular quantum number J ,
- (2) the rotational quantum number R , related to the "pure" rotational momentum $\vec{R} = \vec{J} - \vec{l}$, where \vec{l} is the vibrational angular momentum,
- (3) the symmetry C of the level (with respect to T_d),
- (4) and a multiplicity index n , appearing when several levels have the same symmetry C , for given J and R , that is when the representation $D^{(R)}$ of $O(3)$ contains C several times in its reduction in T_d . Note that all works following Moret-Bailly's notations have n starting from zero, and use a condensed index $p = (C, n)$.

The tensor Hamiltonian may be developed to any order of approximation, defined

by the order of magnitude of the last contribution to the energy. The original work (34) gave a development to fourth order; it was then extended to the sixth order by Michelot *et al.* (36), from which we take the present notations.

When the development is performed to the required order, it appears that many operators have proportional matrix elements and can be recast. The effective Hamiltonian, for the given vibrational state, is then a linear combination of independent operators:

$$\mathbf{H} = \sum_k c_k \mathbf{H}_k \quad (19)$$

where the \mathbf{H}_k operators are adapted to the symmetry of the molecule, whereas the numerical parameters c_k depend on its physical nature. The analytical problem is thus to derive the values of these "effective molecular constants" c_k from the experimental measurements of transition frequencies.

III.B. The Fifth-Order Expansion of the Hamiltonian

In previous works on spherical tops using the present formalism, the development of the Hamiltonian to third or fourth order was generally sufficient to give numerical results in excellent agreement with the experimental accuracy. In the case of heavy molecules, at very high resolution, an expansion to a higher order is necessary, especially when very-high-resolution techniques are used to measure frequencies, such as saturated absorption spectroscopy. In the present analysis, we decided to retain a fifth-order expansion, taking into account the very high accuracy of the data but also their rather small number. We shall see that this choice has been completely justified a posteriori.

So, to the fifth order of approximation, the matrix elements of the Hamiltonian for the excited F_2 vibrational state (ν_3 or ν_4 in the single-level approach) are given by the following formula, where the quantum numbers are written in short $\langle (q.n.) \rangle = \langle J; \nu_3 = 1, l_3 = 1; R, p \rangle$:

$$\begin{aligned} \langle (q.n.) | \mathbf{H} | (q.n.)' \rangle = & [\alpha + \beta J(J+1) + \gamma J^2(J+1)^2 + \pi J^3(J+1)^3] \Delta(R, p) \\ & + 3\sqrt{2}[\lambda + \chi J(J+1) + a_5 J^2(J+1)^2] \{101\} (2R+1)^{1/2} f(J, 0, 2) \Delta(R, p) \\ & + 5\sqrt{6}[\delta + \psi J(J+1)] \{202\} (2R+1)^{1/2} f(J, 1, 3) \Delta(R, p) + \{3\sqrt{3}[\epsilon + \rho J(J+1)] \{044\} \\ & \times f(J, 3, 5) + 5\sqrt{21}[\varphi + \sigma J(J+1)] \{242\} f(J, 1, 3) + 3\sqrt{42}[\mu - b_5 J(J+1)] \{143\} \\ & \times f(J, 2, 4) + 15\sqrt{231/2} \tau \{244\} f(J, 3, 5) + (3\sqrt{33}/2\sqrt{10}) c_5 \{145\} f(J, 4, 6) \} \\ & \times [(2R+1)(2R'+1)]^{1/2} (-1)^{R(i)} (-1)^{R-R'} \mathbf{F}_{A_1, p' p}^{(4 R' R)} + \{\sqrt{39} \xi \{066\} f(J, 5, 7) + \sqrt{858} \eta \{264\} \\ & \times f(J, 5, 7) - (\sqrt{143}/2) d_5 \{165\} f(J, 4, 6)\} [(2R+1)(2R'+1)]^{1/2} (-1)^{R(i)} (-1)^{R-R'} \mathbf{F}_{A_1, p' p}^{(6 R' R)}. \quad (20) \end{aligned}$$

For simplicity we have set the following condensed notations:

$$\Delta(R, p) = \begin{cases} 1 & \text{if } R' = R \quad \text{and} \quad p' = p \\ 0 & \text{otherwise} \end{cases}$$

$$f(J, m, n) = [(2J-m)(2J-m+1) \cdots (2J+n)]^{1/2}$$

and the $9 - j$ symbol

$$\{abc\} = \begin{Bmatrix} a & b & c \\ 1 & R & J \\ 1 & R' & J \end{Bmatrix}.$$

The $F_{A_1 P' P}^{(n R' R)}$, with $n = 4$ and 6 , were first computed by Moret-Bailly *et al.* (37) for low J 's, then up to very-high- J values by Krohn (38). Let us recall that the $F^{(4)}$ symbols are diagonal in p when they are diagonal in R , but this is not the case for the $F^{(6)}$ ones, and that both symbols are pure imaginary numbers when $(R' - R)$ is odd (which explains the phase factor $(i)^R$ used to make the Hamiltonian matrix real).

Similarly, in the ground state ($v_s = 0$, all s) the Hamiltonian is not completely diagonal with respect to the chosen basis, and its matrix elements are

$$\begin{aligned} \langle J_0; v_s = 0; J_0, p_0 | \mathbf{H} | J_0; v_s = 0; J_0, p_0' \rangle \\ = [\beta_0 J_0 (J_0 + 1) + \gamma_0 J_0^2 (J_0 + 1)^2 + \pi_0 J_0^3 (J_0 + 1)^3] \Delta(J_0, p_0) \\ + [\epsilon_0 + \rho_0 J_0 (J_0 + 1)] f(J_0, 3, 5) (-1)^{J_0} F_{A_1 p_0 p_0}^{(4 J_0 J_0)} + \xi_0 f(J_0, 5, 7) (-1)^{J_0} F_{A_1 p_0 p_0}^{(6 J_0 J_0)} \quad (21) \end{aligned}$$

using the same notations as above.

Up to the fifth order of approximation, we thus have 20 molecular constants to describe the excited ($v_3 = 1$) state, and 6 for the ground state. Some of these constants are directly related to physical parameters. For instance:

- (1) α is the vibrational energy,
- (2) β and γ (resp., β_0 and γ_0) are the inertial and the scalar centrifugal distortion constants in the excited (resp., ground) state,
- (3) λ is connected with the Coriolis coupling coefficient ζ_3 by

$$\lambda = -\beta \zeta_3. \quad (22)$$

For most constants occurring in low-order terms of the Hamiltonian, relationships can be established with the parameters used in other formalisms. For example, we give in Table I the connection with the usual notations of Hecht (39); more detail can be found in Ref. (40).

Given a set of adequate molecular constants, the numerical diagonalization of the Hamiltonian matrices (both in the ground and excited states) is performed, leading to eigenvalues which are the rovibrational energies in both states. Thus the frequencies of the allowed transitions are simply obtained by subtractions, according to the selection rules. In the usual case where internal mixing is not too important, the selection rules given by the general formula (12) are

- (a) $\Delta C = 0$
- (b) $\Delta J = J - J_0 = -1, 0, +1$, giving rise, respectively, to the P , Q , and R branches,
- (c) $\Delta R = R - J_0 = 0$
- (d) $\Delta n = n - n_0 = 0$.

Yet, it must be kept in mind that the last two rules are not strict and that, in many cases, "forbidden" lines do appear (which may bring valuable information, as will be specified later).

Since a triply degenerate F_2 level ($v_3 = 1$) is characterized by the vibrational angular quantum number $l_3 = 1$, we have then $R = J, J \pm 1$, and, as a consequence of the

TABLE I
Effective Molecular Constants for the Ground and ($\nu_3 = 1$) States of $^{32}\text{SF}_6$,
up to the Fifth Order of Approximation

Ord.	Molecular constant		Numerical value (standard deviation)	
	J.M.B.	K.T.H.	in MHz	in cm^{-1} **
S0	B_0	B_0	$2.730635624(31) \times 10^3$	$9.10842001(10) \times 10^{-2}$
S2	γ_0	$-D_{S0}$	$-1.66308(13) \times 10^{-4}$	$-5.54743(43) \times 10^{-9}$
S4	π_0		$-3.2186(13) \times 10^{-9}$	$-1.07362(43) \times 10^{-13}$
T2	c_0	$-(\sqrt{3}/2\sqrt{7})D_{40}$	$1.86383(63) \times 10^{-6}$	$6.2171(21) \times 10^{-11}$
T4	ρ_0	$-(\sqrt{3}/2\sqrt{7})H_{40}$	$9.9206(91) \times 10^{-11}$	$3.3091(30) \times 10^{-15}$
T4	ξ_0	$-(1/16\sqrt{2})H_{60}$	$-1.757(10) \times 10^{-12}$	$-5.860(33) \times 10^{-17}$
S0	α	ν	$28.423398592(12) \times 10^6$	$948.10252337(40)$
S2*	$\Delta B = B_3 - B_0$	$\Delta B = B_3 - B_0$	$-3.928945(21)$	$-1.3105551(70) \times 10^{-4}$
S4*	$\Delta \gamma = \gamma_3 - \gamma_0$	$-(D_S - D_{S0})$	$-1.243(14) \times 10^{-6}$	$-4.147(48) \times 10^{-11}$
S5*	$\Delta \pi = \pi_3 - \pi_0$		$-6.23(23) \times 10^{-11}$	$-2.077(79) \times 10^{-15}$
S1	λ	$-(B\epsilon)_3$	$-1.89081685(51) \times 10^{-3}$	$-6.3070861(17) \times 10^{-2}$
S2	δ	$-(1/12)Z_S$	$-2.290804(25) \times 10^{-1}$	$-7.641299(85) \times 10^{-6}$
S3	χ	$(1/2)F_S$	$4.7899(56) \times 10^{-4}$	$1.5977(19) \times 10^{-8}$
S4	ψ		$-1.7942(76) \times 10^{-7}$	$-5.985(25) \times 10^{-12}$
S5	a_5		$1.7321(85) \times 10^{-8}$	$5.778(29) \times 10^{-13}$
T4*	$\Delta \epsilon = \epsilon_3 - \epsilon_0$	$-(\sqrt{3}/2\sqrt{7})\Delta D_t$	$-9.774(65) \times 10^{-8}$	$-3.260(22) \times 10^{-12}$
T2	φ	$-(\sqrt{3}/\sqrt{7})Z_t$	$-7.36639(10) \times 10^{-1}$	$-2.457163(35) \times 10^{-5}$
T3	μ	$(\sqrt{3}/2\sqrt{7})F_t$	$-2.516(32) \times 10^{-6}$	$-8.39(11) \times 10^{-11}$
T4	σ		$-1.752(45) \times 10^{-7}$	$-5.84(15) \times 10^{-12}$
T4	τ		0.0 †	0.0 †
T5*	$\Delta \rho = \rho_3 - \rho_0$		$-5.7(14) \times 10^{-13}$	$-1.90(49) \times 10^{-17}$
T5	b_5		$3.676(94) \times 10^{-10}$	$1.226(32) \times 10^{-14}$
T5	c_5		0.0 †	0.0 †
T5*	$\Delta \xi = \xi_3 - \xi_0$		$-1.141(32) \times 10^{-12}$	$-3.81(11) \times 10^{-17}$
T4	η		$1.446(33) \times 10^{-12}$	$4.82(11) \times 10^{-17}$
T5	d_5		$4.053(10) \times 10^{-10}$	$1.3519(34) \times 10^{-14}$

Note. We give the notation of Moret-Bailly (J.M.B.) used in this paper and, whenever possible, the correspondence with Hecht's formalism (K.T.H.), together with the indication of the nature (S = scalar, T = tensor) and order of magnitude of the first operator connected with the constant. All standard deviations within parentheses (99% confidence intervals) are in units of the last quoted digit.

* See footnote 7.

** Given $c = 299\,792\,458$ m/sec.

† Fixed to zero (see text).

above selection rules, each fine level of the excited state may be reached by one and only one "allowed" transition from the ground state. This explains why each fine structure of the spectrum reproduces exactly the structure of the related group of energy levels. These structures are very characteristic of spherical tops and are called "tetrahedral" fine structures.

Now, to close this subsection, we have to be a little more explicit about the application of the present formalism to the case of XY_6 molecules:

The symmetry group of XY_6 octahedral molecules is O_h which has 10 irreducible

representations (their notations are obtained from those of T_d by adding the parity index u or g). Among the six normal modes of vibration, only ν_3 and ν_4 are (strictly speaking) infrared active, because they are of symmetry F_{1u} . The ground vibrational state is of symmetry A_{1g} .

It is well known, and has been clearly established by Michelot (35), that

(i) in a given vibrational state, two eigenfunctions which differ only by the parity index (u or g) lead to the same rovibrational energy (this degeneracy is removed only by the hyperfine interactions);

(ii) these energies can be obtained from a rovibrational Hamiltonian which is formally identical to the one used for XY_4 tetrahedral molecules, given a simple correspondence between vibrational symmetry labels, for example: $F_{1u}(O_h) \rightarrow F_2(T_d)$, and $A_{1g}(O_h) \rightarrow A_1(T_d)$.

So, from the rovibrational point of view (disconnected from the hyperfine problem), we can use for a F_{1u} (resp., A_{1g}) vibrational level of XY_6 spherical tops the same formalism and formulae as for a F_2 (resp., A_1) vibrational level of XY_4 molecules. Yet, we must keep in mind that, in this case, a given rovibrational symmetry label C covers two degenerate states C_g and C_u , except for rovibrational labels A_2 , E , and F_2 (because A_{2g} , E_g , and F_{2u} are strictly forbidden by the Pauli principle).

As a consequence, the "effective" spin statistical weights $g_S(C)$ we have to consider in the rovibrational problem for SF_6 (or any XY_6 octahedral top with nuclear spins $i_X = 0$ and $i_Y = \frac{1}{2}$) take the following values:

symmetry:	A_1	A_2	E	F_1	F_2
$g_S(C)$:	$1 + 1 = 2$	$10 + 0 = 10$	$8 + 0 = 8$	$3 + 3 = 6$	$6 + 0 = 6$

These values are to be used for the calculation of the intensities of rovibrational transitions, according to the general theory described in Subsection II.B.2.

III.C. The Use of Spectroscopic "Band Parameters"

For a long time, the lack of powerful computational tools, and also the comparative mediocrity of experimental accuracy, have led to the use of approximate perturbation methods in the determination of energy levels of spherical tops. The Hamiltonian of Moret-Bailly is especially well adapted to this purpose because, in the case of F_2 (or F_{1u}) vibrational states, it is almost diagonal. So, it is possible to get a rough estimate of the eigenvalues simply by keeping the diagonal matrix elements. Though this method has not been used in the present paper, we feel it is interesting to recall here its main features, essentially with the purpose of showing the limits of such an approximate procedure.

Using the general matrix elements of Eqs. (20) and (21) and the selection rules, the diagonal contribution to the transition frequencies can be written in the form introduced by Bobin and Fox (41); for the P and R branches we have

$$f_{PR}(R, p) = m + nX + pX^2 + qX^3 + sX^4 + tX^5 + xX^6$$

$$+ [g + hX + kX^2 + lX^3 + jX^4] \frac{(-1)^R}{A(X)} \mathbf{F}_{A_1 PP}^{(4RR)} + [z' + z''X + z'''X^2] \frac{(-1)^R}{A'(X)} \mathbf{F}_{A_1 PP}^{(6RR)} \quad (23)$$

where $X = R + 1$ and $X = -R$ for the R and P branches, respectively.

For the Q branch we have

$$f_Q(R, p) = m + vR(R+1) + wR^2(R+1)^2 + xR^3(R+1)^3 - [2g - uR(R+1) - zR^2(R+1)^2] \frac{(-1)^R}{B(R)} F_{A_1 p p}^{(4 R R)} - [2z' - z''R(R+1)] \frac{(-1)^R}{B'(R)} F_{A_1 p p}^{(6 R R)}. \quad (24)$$

In these expressions, which are valid up to the fifth order of approximation, we have defined

$$A(X) = 2X(2X+1)/[(-1)^X(2X-5) \cdots (2X+3)]^{1/2}$$

$$A'(X) = 2X(2X+1)/[(-1)^X(2X-7) \cdots (2X+5)]^{1/2}$$

$$B(X) = 2X(2X+2)/[(2X-3) \cdots (2X+5)]^{1/2}$$

$$B'(X) = 2X(2X+2)/[(2X-5) \cdots (2X+7)]^{1/2}.$$

The numerical parameters m, n, p, \dots , are linear combinations of the molecular constants related to the ground and the excited states: we call them spectroscopic "band parameters." Their appropriate expressions, up to the fifth order of approximation, are given in Table II. We must point out that this "order of approximation" is defined with respect to the order of expansion of the Hamiltonian, and is related to the order of magnitude of the last contribution to the rovibrational energy. There is generally no simple connection between the order of approximation and the degree

TABLE II

Spectroscopic Band Parameters for ν_3 of $^{32}\text{SF}_6$, Calculated from Their Expressions in Terms of the Molecular Constants (Last Column), and Using the Numerical Values of Table I

Param.	Value (s.d.) in cm^{-1}	Combination of constants
m	947.97633577(43)	$\alpha + 2\lambda + 6\delta$
n	$5.5819241(38) \times 10^{-2}$	$\beta + \beta_0 + 2\lambda + 10\delta + 2\chi + 6\psi$
p	$-1.615569(11) \times 10^{-4}$	$\beta - \beta_0 + \gamma - \gamma_0 + 4\delta + 4\chi + 16\psi + 2a_5$
q	$9.602(40) \times 10^{-9}$	$2\gamma + 2\gamma_0 + \pi + \pi_0 + 2\chi + 14\psi + 6a_5$
s	$-6.195(60) \times 10^{-11}$	$\gamma - \gamma_0 + 3\pi - 3\pi_0 + 4\psi + 6a_5$
t	$5.051(62) \times 10^{-13}$	$3\pi + 3\pi_0 + 2a_5$
x	$-2.077(79) \times 10^{-15}$	$\pi - \pi_0$
v	$-6.9893200(61) \times 10^{-5}$	$\beta - \beta_0 - 8\delta + 2\chi + 6\psi$
w	$7.56(28) \times 10^{-12}$	$\gamma - \gamma_0 - 8\chi + 2a_5$
g	$-2.456978(34) \times 10^{-5}$	$\varphi + 20\epsilon - 8\mu - 100\tau + 30c_5$
h	$-1.2660(34) \times 10^{-9}$	$-18\epsilon + 2\epsilon_0 - 20\rho + 4\mu - \sigma + 90\tau - 2b_5 - 37c_5$
k	$-1.872(24) \times 10^{-11}$	$38\rho + 2\rho_0 + 4\epsilon - 4\epsilon_0 + \sigma - 20\tau + 3b_5 + 15c_5$
l	$9.126(50) \times 10^{-14}$	$22\rho + 2\rho_0 + b_5 + 4c_5$
$j=z$	$-7.6(1.9) \times 10^{-17}$	$4\rho - 4\rho_0$
u	$-1.54(21) \times 10^{-12}$	$4\epsilon - 4\epsilon_0 - 40\rho - 2\sigma + 40\tau - 4b_5 + 10c_5$
z'	$3.654(16) \times 10^{-14}$	$42\xi + \eta + 3d_5$
z''	$1.1122(70) \times 10^{-14}$	$26\xi - 2\xi_n + d_5$
z'''	$-1.523(43) \times 10^{-16}$	$4\xi - 4\xi_0$

Note. The parameters j and z are equal at the fifth order of approximation. All values and derived standard deviations are in cm^{-1} . Please refer to the text (Sect. III.C) for a correct use of these parameters.

in J (or R) of the polynomials occurring in Eqs. (23) and (24). For instance the main rotational operator (related to the rigid rotator) appears in the zeroth-order Hamiltonian, but gives a contribution to the energy proportional to $J(J + 1)$, and then contributes to the parameters n and p (or v in the Q branch).

In this diagonal approximation, the terms involving the $F^{(6)}$ being generally small, it is obvious that the positions of the lines within an R manifold are proportional to the $F^{(4)}$ symbols. The usual assignment method follows directly from this remarkable property (as far as fine structures do not overlap too much). Approximate values of the band parameters can then be deduced from the frequencies of the transitions, using for instance a least-squares calculation. A refinement is obtained by introducing corrections to the diagonal terms, usually by a first- or second-order perturbation method (or, sometimes, more sophisticated procedures). Yet, and this is the most important point we want to emphasize, the expressions of off-diagonal corrections that can be calculated (34, 41) involve new linear combinations of molecular constants; these "off-diagonal parameters" cannot be connected simply to the parameters g , h , So, only approximate expressions of the off-diagonal corrections can be written in terms of the diagonal parameters (the only ones that can be deduced from the calculation). With the expressions given in Refs. (34, 41), the corrections are valid only up to the third order of approximation.⁶

So, it appears that, finally, such an approximate procedure is valid only up to the third order of approximation, and that it would be inconsistent to try to determine more than the seven parameters appearing up to this order, namely m , n , p , q , v , g , and h (any other higher order parameter numerically derived from the analysis of the spectrum would not keep its true physical significance). Let us add that, as it is well known by people using this procedure, it is impossible to derive significant values of all the molecular constants from the band parameters only (even if the constants of the ground state are known).

Nevertheless, to moderate somehow the severe criticism that we seem to bring not against the method, but against the often use of this method, we must say that this approximate procedure can be extremely useful in starting the analysis of a band, especially with low-resolution spectra, and also in extrapolating the calculations to very-high- J values (when the dimensions of the true Hamiltonian matrices become too large to reasonably proceed by exact diagonalization).

The reader has probably already understood that if we want to treat the problem properly, it is necessary to come back to the exact expression of the rovibrational Hamiltonian, Eqs. (20) and (21), and to use a more adequate numerical procedure, especially if we want to reach the accuracy of saturation spectra.

III.D. Determination of the Molecular Constants

In previous analyses of the ν_3 band of SF_6 (42–45, 7) approximate numerical methods were generally used, more or less similar to the one described in the preceding sub-

⁶ We thank Krohn (60) for having drawn our attention to an error in the expression of the $(J, J + 1)$ off-diagonal term given by Moret-Bailly, Eq. (204) of (34) or Eq. (13) of (61). This term should read: $[(\varphi + 12\epsilon - 6\mu) - J(8\epsilon - 2\mu)]$ instead of $[(\varphi - 12\epsilon + 6\mu) + J(8\epsilon - 2\mu)]$, so that the off-diagonal terms can all be expressed in terms of diagonal band parameters up to the third order of approximation. The reader will also find new interesting expressions of the line frequencies in a first- or second-order perturbation approximation in the papers by Krohn and Watson (62).

section. The final standard deviation on the fitted lines was always much larger (by one or two orders of magnitude) than the experimental accuracy. So we decided to completely reconsider the problem, in order to reach an accuracy of the theoretical model close to the accuracy of the saturated absorption measurements. First, it is necessary to come back to the complete expansion of the vibration-rotation Hamiltonian, developed to the fifth order of approximation in the present case.

According to Eqs. (19)–(21), this Hamiltonian can be written, respectively, in the ground and excited states as

$$\mathbf{H}_0 = \sum_k c_{0k} \mathbf{H}_{0k} \quad (25)$$

and

$$\mathbf{H}_3 = \sum_l c_{3l} \mathbf{H}_{3l} \quad (26)$$

were the c_{0k} and c_{3l} are the molecular constants of the two levels, to be determined. The matrix elements of the \mathbf{H}_{0k} and \mathbf{H}_{3l} operators are calculated once and for all, and stored on a magnetic tape, for all needed values of J_0 and J . For example, they are directly put into (J, C) blocks for the ν_3 level (up to $J = 95$ in the present analysis).

From these matrix elements and for a given set of molecular constants, a second computer program builds the Hamiltonian matrices of the excited ($\nu_3 = 1$) state (by blocks (J, C)) and of the related ground states (the three blocks $(J_0 = J, J \pm 1; C)$). A full diagonalization of both the excited and the ground state matrices is performed, leading to the eigenvalues and the eigenvectors. The frequencies of allowed transitions are then calculated by differences corresponding to the selection rules (and, if required, of all possible “forbidden” transitions), together with their intensities at a given temperature.

These computed frequencies have to be compared to the experimental ones, in order to derive corrections to the initial set of molecular constants. This is achieved using a linearization of the problem and a least-squares technique:

Let \mathbf{T} be the matrix of eigenvectors which diagonalize the Hamiltonian matrix \mathbf{H} (either \mathbf{H}_0 or \mathbf{H}_3). Then the transformed matrix \mathbf{E} :

$$\mathbf{E} = \mathbf{T}^{-1} \mathbf{H} \mathbf{T} \quad (27)$$

is diagonal, and its nonzero elements are the energies of the related state. Using Eq. (25) and introducing transformed operators \mathbf{H}'_{0k} , we can write the following equations:

$$\begin{aligned} \mathbf{E}_0 &= \mathbf{T}_0^{-1} \left[\sum_k c_{0k} \mathbf{H}_{0k} \right] \mathbf{T}_0 = \sum_k c_{0k} [\mathbf{T}_0^{-1} \mathbf{H}_{0k} \mathbf{T}_0] \\ &= \sum_k c_{0k} \mathbf{H}'_{0k} \end{aligned} \quad (28)$$

for the ground state, and similar equations for the ν_3 state. Then the i th eigenvalue, in this state, can be estimated as the linear combination:

$$E_{0i} = \sum_k c_{0k} [\mathbf{H}'_{0k}]_i \quad (29)$$

and the frequency of the transition from this ground state level to the j th level of the ν_3 state is

$$\nu_{ij} = E_{3j} - E_{0i} = \sum_l c_{3l} [\mathbf{H}_{3l}]_j^i - \sum_k c_{0k} [\mathbf{H}_{0k}]_i^j. \quad (30)$$

If ν_{obs} is the observed frequency for this transition, then the difference $\nu_{ij} - \nu_{\text{obs}}$ is a linear combination of the corrections δc_{0k} and δc_{3l} to apply to the initial set of molecular constants, in order to get a better agreement between the observed and computed values. As far as the number of experimental data is at least equal to (and in practice much larger than) the number of molecular constants, these corrections can be derived, together with their standard deviations (confidence intervals), using the well-known least-squares method.

This procedure can be repeated as many times as required. In practice it is stopped when all the corrections on the molecular constants become smaller than half the corresponding standard deviations. The standard value of the deviations between computed and observed frequencies has, in the same time, become minimal (its possible fluctuations are no longer significant). Note also that it is always possible, during the iterative procedure, to fix any molecular constant to a given value (or, in more refined programs, to tie it down to a given variation interval). Besides, the program takes care of the case where a difference (observed – computed) in frequencies appears to be abnormally large (with respect to the standard deviation of the fit): an adjustable test will eliminate the corresponding line from the computation.

From this brief description of the numerical procedure, it appears that it would be possible to determine all the molecular constants which are involved in the Hamiltonian expansion. The reality is of course slightly different, because some operators which occur both for the ground and for the excited states happen to have equal matrix elements in the two states, for $J_0 = R$; these scalar operators are related to the constants noted β , γ , and π . Because of this property and of the selection rule $\Delta R = R - J_0 = 0$, the frequencies of allowed transitions depend exactly in the same manner of the molecular constants in both states, and more precisely of their differences only, for example, $\beta_3 - \beta_0$ for the main rotational operator. This is the reason why it is generally said that it is impossible to fit simultaneously the ground and the excited states only from the frequencies of “allowed” transitions of a fundamental band. This difficulty would be removed by the observation of “forbidden” lines, that is with $\Delta R \neq 0$ and $\Delta n \neq 0$. Unfortunately, in the case of ν_3 of SF_6 , the intensities of such transitions are so weak that it is extremely difficult to detect them.

Yet, there is a way to get around this difficulty. Let us consider, for example, the main rotational operator, which gives the energy contributions $\beta_3 J(J+1)$ and $\beta_0 J_0(J_0+1)$ in the excited and ground states, respectively. From the Hamiltonian construction, we know that the difference $\Delta\beta = \beta_3 - \beta_0$ is small compared to β_0 . Then, rather than introducing the operators related to β_3 and β_0 , we can introduce one with β_0 in both states and one with $\Delta\beta$ in the ($v_3 = 1$) state. If the constant β_0 is unknown, or simply roughly estimated, we can fix to zero the “correction” $\Delta\beta$ in a first set of iterations, and get a first (or better) evaluation of β_0 . Then, in a second set of iterations, we fix β_0 to the value obtained, and can get a first estimation of $\Delta\beta$, and so on, by successively fixing β_0 or its correction $\Delta\beta$ to the ($v_3 = 1$) state. This procedure can be simultaneously applied to the three scalar constants β , γ , and π . It converges after a rather small number of sets of iterations, depending on the initial estimation of the constants, on the relative values of the corrections in the excited state, and also on the accuracy of

the experimental data. For SF_6 , as will be seen in the next subsection, very accurate values have been derived after only five sets of five to six iterations.

Now, concerning the tensor operators which occur both in the ground and excited states, namely those related to the constants ϵ , ρ , and ξ , there is no problem, in principle, for the following reason: though the matrix elements of these operators are equal in the ground and excited states (for given J_0 and $R = J_0$), their exact contributions to the transition frequencies are no longer equal after the bases change, Eqs. (28)–(30), simply because the \mathbf{T} matrices are different in the two states. Yet, these operators being generally almost diagonal (especially for heavy spherical tops), the difference between the two contributions will be significant, in the numerical computation, only when experimental frequencies are measured with a very high accuracy. Then the possibility to consider such constants as ϵ_3 and ϵ_0 (or ρ_3 and ρ_0 , or else ξ_3 and ξ_0) as linearly independent is highly dependent on the experimental precision. When this opportunity is not given, we still have the possibility to use the same iterative procedure as for the scalar constants β , γ , and π .

To close this section, let us recall that it has recently been proved by Tyuterev *et al.* (46) that, when we restrict the general tensor Hamiltonian (whatever the formalism is) to a given vibrational problem (here $\nu_3 = 1$), and to a given order of development, this leads to some ambiguity for the “effective” molecular constants which are numerically derived; indeed the solution is not unique or, in other words, all involved molecular constants are not necessarily linearly independent. In the case of Moret-Bailly’s Hamiltonian, presently used, these authors have shown that there is a linear relationship between the constants σ and τ , on one hand, and b_5 and c_5 , on the other hand. Since there is (as far as we know) no logical reason to choose one rather than the other, we decided for the present work to arbitrarily fix to zero the two constants τ and c_5 (let us recall that this choice has no influence at all on the numerical fit of the frequencies). Then, for the present problem, we shall retain 18 effective molecular constants for the ($\nu_3 = 1$) vibrational state, together with the 6 ones of the ground state.

IV. ROVIBRATIONAL ANALYSIS OF ν_3 OF SF_6

We have applied the formalism and the numerical method described in Section III to the 136 measured transitions of ν_3 of SF_6 , using the frequencies obtained after deconvolution of the fine structures (except for the 11 lines where the N_2O laser is involved), as explained in Section II. First, let us mention that the rovibrational assignments of these lines were already known both from previous analyses and from hyperfine studies, and have been confirmed as a whole.

IV.A. Effective Molecular Constants

In order to start the iterative procedure described in Subsection III.D, a preliminary estimate of the main molecular constants was needed. This was achieved by using the last published values of the band parameters of Ref. (7), and also some experimental or theoretical estimates of the ground state constants: $\beta_0 = \text{B}_0 = 0.091084(2) \text{ cm}^{-1}$ was given by Patterson *et al.* (47); ϵ_0 may be deduced from the value of $t_{044} = -D_t = 5.7(0.7) \text{ Hz}$ observed by Bordé *et al.* (7, 21), which leads to $\epsilon_0 = 1.86(23) \text{ Hz}$; and

a theoretical estimate of $\gamma_0 = -D_s = -6.36(7) \times 10^{-9} \text{ cm}^{-1}$ has been calculated by Berger and Aboumajd (48).

The other ground state constants π_0 , ρ_0 , and ξ_0 were first estimated by setting to zero their corrections ($\Delta\pi$, $\Delta\rho$, and $\Delta\xi$) in the ($v_3 = 1$) state. Then, as described in Subsection III.D, it was possible, with the help of the very high accuracy of the measured frequencies (5 kHz), to have a direct estimate of all tensorial constants, both in the ground and excited states. The scalar constants β_0 , γ_0 , and π_0 were also refined, together with their "corrections" in the ($v_3 = 1$) state, using the procedure described in III.D.

Finally, we got significant values for all constants involved in the fifth-order Hamiltonian expansion. They are presented in Table I (in MHz and cm^{-1}), together with their standard deviations (99% confidence intervals, in units of the last quoted digit). When possible we recall the corresponding notation of the constant in the usual Hecht's formalism. Besides, in order to facilitate the comparison with other studies, we also indicate the nature (scalar or tensorial) of the operator leading to the given constant, together with the order in the Hamiltonian expansion where the first contribution to the constant occurs.⁷

Some important spectroscopic parameters can be deduced from the present molecular constants. In particular the Coriolis coupling coefficient ζ_3 takes the value

$$\zeta_3 = -\lambda/\beta_3 = 0.69344341(20)$$

and a better evaluation of the S-F bond length in the ground state can be derived from β_0 , leading to

$$r_0(\text{S-F}) = 1.5605(3) \text{ \AA}.$$

Let us give a few remarks about these numerical results:

(a) All molecular constants have meaningful values, which justifies the use of a fifth-order expansion for the Hamiltonian; yet the constants $\Delta\rho$ and $\Delta\pi$ (which are indeed of the fifth order) are barely meaningful which means that higher order terms (from a sixth-order expansion) would probably not bring any valuable improvement.

(b) The determination of accurate values of the ground state constants for heavy spherical tops, only from allowed transitions of a fundamental band, has always been a tough problem. Though some results have been obtained for the main rotational constant B_0 for SF_6 (63) or UF_6 (64), for example, the present analysis is, as far as we know, the first attempt to evaluate all the molecular constants with very high accuracy. Moreover, the values obtained are in good agreement with the theoretical or experimental estimates which have been mentioned above.

(c) As will be detailed in the next subsection, these values are derived from a fit including only 128 among the 136 available observed transitions (those with deviations less than 100 kHz). But it is remarkable that such accurate values can be obtained from about only one percent of all the allowed transitions in the studied spectral range (11 520 up to $J = 95$). This can be explained both by the extreme accuracy of the experimental frequencies, and by the use in the numerical fit of transitions from the P , Q , and R branches, with almost regularly spaced J values, from $J = 2$ to 95 (this point resulting from a good sampling by successive laser lines).

⁷ It must be noted that, though β_3 and β_0 result from zeroth-order operators, their difference $\Delta\beta$ comes from second-order terms. Similarly, $\Delta\gamma$ and $\Delta\epsilon$ must be considered as fourth-order constants, whereas $\Delta\pi$, $\Delta\rho$, and $\Delta\xi$ are of fifth order.

In order to make the comparison with the most recently published analyses of this band (45, 7), we give in Table II the values of the spectroscopic band parameters, Eqs. (23) and (24), that can be *calculated* from our molecular constants, together with the adequate expressions of these parameters (up to the fifth order). This might be also of some interest to anyone willing to extrapolate the present rovibrational analysis to higher J values (in the diagonal approximation, as explained in Subsect. III.C).

Let us add that, considering the standard deviations on the molecular constants, the absolute values of vibration-rotation energies are computed with a mean precision of 0.185 MHz in the ground state and 0.380 MHz in the ($\nu_3 = 1$) state, for $J = 50$, and, respectively, around 2.35 and 5.45 MHz for $J = 95$ (of course the accuracy on differences, that is, on the frequencies, is much better, as will be discussed below). A complete listing of the rovibrational energy levels, both in the ground and the ($\nu_3 = 1$) states, can be obtained upon request.

IV.B. The Fit of Saturated Absorption Frequencies

The comparison between our final computed frequencies, using the molecular constants of Table I, and the measured frequencies (as defined in Sect. II) used as data, is presented in Table III. For each studied spectral range (each laser line) the observed resonances of SF_6 are listed with the following data:

- (1) the assignment of the SF_6 ν_3 rovibrational transition (branch, J_0 , C_0 and n_0),
- (2) the final measured frequency (in MHz), after deconvolution of the fine structure from the hyperfine structures,
- (3) the difference (observed - computed) in frequencies (in MHz).

The fit from which the molecular constants have been deduced includes only the 128 lines with deviations less than 0.100 MHz; the 8 remaining lines are indicated in Table III by a special mark (<). The standard deviation⁸ of this fit is

$$\sigma_d = 0.028 \text{ MHz} = 0.93 \times 10^{-6} \text{ cm}^{-1}$$

which is close to the experimental accuracy, and represents a considerable improvement with regard to previous analyses. If we include the remaining lines in the calculation of σ_d (without changing the molecular constants), its value raises up to 0.314 MHz. We could also try a new fit including all the 136 transitions and leading to somewhat different molecular constants; the new standard deviation on frequencies would be 0.172 MHz. Yet, for the reasons that we explain below, we think that the set of molecular constants given in Table I leads to more consistent and reliable results.

First, let us note that, except for the problem of lines outside the fit, the deviations between observed and computed frequencies do not show significant fluctuations from one laser line to another, even for the $R(10)$ line of the N_2O laser, which is good evidence of the self-consistency of the measurements. Besides, these deviations show no more dependence on the quantum number J , even for the highest values, which confirms, once more, that the Hamiltonian expansion has been performed up to a sufficient order of approximation.

⁸ Let us recall that the unweighted standard deviation σ_d which is used here is defined as $\sigma_d = [(\sum(\nu_{\text{cal}} - \nu_{\text{obs}})^2)/(N - p)]^{1/2}$, where N is the number of involved data, and p the number of constants derived from the fit ($N - p$ is then the number of independent data). In our final numerical fit, we had $N = 128$ and $p = 24$.

TABLE III

Comparison of Computed and Observed Frequencies for the 136 Transitions of ν_3 of $^{32}\text{SF}_6$
Measured by Saturation Spectroscopy

Notes to the Table:			Coincidences with P16 of CO_2		Coincidences with P14 of CO_2			
(a) These observed frequencies are not corrected of hyperfine effects (see the text).								
(<) Transition outside the fit (deviation larger than 0.10 MHz)								
Coincidences with P22 of CO_2			Q 55 F2(6)	28412340.258	0.017	R 28 F1(2)	28464417.830	0.014
P 83 F1(13)	28251749.116	0.484<	Q 55 F1(6)	28412347.656	0.037	R 28 E (1)	28464506.923	0.034
P 82 F2(10)	28251854.218	0.037	Q 46 F1(3)	28412376.486	-0.038	R 28 F2(2)	28464529.560	0.035
P 82 F1(10)	28251856.339	0.014	Q 49 F1(7)	28412382.721	0.040	R 28 A2(0)	28464691.306	0.016
P 81 F1(8)	28251999.598	-0.008	Q 47 F1(7)	28412397.039	0.014	R 28 F2(1)	28464712.420	0.024
P 81 F2(7)	28251999.615	-0.009	Q 49 E (4)	28412430.671	0.052	R 28 F1(1)	28464728.434	0.029
P 84 A2(1)	28252005.614	0.006	Q 54 A2(2)	28412442.814	-0.011	R 28 A1(0)	28464741.935	0.031
P 84 F2(3)	28252005.891	0.003	Q 54 F2(7)	28412452.980	0.010	R 29 F1(2)	28464858.047	-0.085
P 84 F1(3)	28252006.168	0.000	Q 54 E (4)	28412457.940	0.021	R 29 F2(1)	28464858.327	-0.085
P 84 A1(1)	28252006.444	-0.003	Q 41 F1(9)	28412467.435	-0.002			
P 83 F2(14)	28252056.358	0.014	Q 41 E (5)	28412472.874	0.000	Coincidences with P12 of CO_2		
P 83 E (9)	28252136.052	-0.046	Q 48 F1(4)	28412474.597	-0.013	R 70 F2(7)	28515795.247	0.044
Coincidences with P20 of CO_2			Q 41 F2(8)	28412478.355	0.002	R 70 F1(7)	28515836.768	0.036
P 57 F1(3)	28305999.064	0.006	Q 45 A2(2)	28412526.411	-0.037	R 72 E (6)	28515843.955	0.010
P 57 F2(3)	28305999.064	0.006	Q 53 F2(6)	28412559.609	-0.014	R 72 F2(10)	28515844.150	0.010
P 58 F2(9)	28306027.542	-0.066	Q 53 F1(6)	28412573.094	0.008	R 72 A2(3)	28515844.541	0.009
P 58 F1(8)	28306027.756	-0.068	Q 38 F2(0)	28412581.959	0.039	R 74 E (8)	28515857.680	0.004
P 59 F1(9)	28306083.696	0.008	Q 38 E (0)	28412582.469	0.042	R 74 F2(12)	28515857.682	0.005
P 60 F1(1)	28306149.748	-1.843<	Q 38 F1(0)	28412582.976	0.039	R 74 A2(3)	28515857.686	0.005
P 60 E (0)	28306149.854	-1.845<	Q 43 P1(8)	28412599.129	-0.032	R 89 A1(0)	28515909.384	-0.003
P 60 F2(1)	28306149.961	-1.846<	Q 45 F2(7)	28412602.224	-0.034	R 89 E (0)	28515909.384	-0.003
P 59 F2(9)	28306151.890	-0.026	Q 48 F2(5)	28412626.007	0.033	R 89 F1(1)	28515909.384	-0.003
P 59 A2(3)	28306252.637	0.102<	Q 43 E (5)	28412626.400	-0.033	R 73 E (4)	28515913.350	0.004
P 55 F2(0)	28306312.965	-0.011	Q 43 F2(8)	28412662.331	-0.024	R 73 F1(7)	28515913.373	0.005
P 55 F1(0)	28306312.965	-0.011	Q 47 E (4)	28412662.561	-0.008	R 73 A1(2)	28515913.416	0.004
P 56 A2(3)	28306352.765	0.022	Q 52 E (4)	28412675.428	-0.020	R 66 A2(0)	28516003.635	-0.003
P 56 E (8)	28306352.765	0.022	Q 52 F1(6)	28412684.371	-0.011	R 66 F2(0)	28516003.636	-0.003
P 56 F2(12)	28306352.765	0.022	Q 46 A1(1)	28412685.722	-0.008	R 66 F1(0)	28516003.637	-0.004
P 59 F2(10)	28306491.162	-0.358<	Q 45 F1(8)	28412689.322	-0.037	R 66 A1(0)	28516003.638	-0.004
Coincidences with P18 of CO_2			Q 52 A1(2)	28412701.510	0.011	R 83 A1(0)	28516052.029	0.009
P 33 F1(5)	28359647.866	-0.003	Q 47 F2(7)	28412736.801	-0.007	R 83 E (1)	28516052.029	0.009
P 32 F2(7)	28359656.406	-0.442<	Q 51 F2(6)	28412795.369	-0.028	R 83 F1(2)	28516052.029	0.009
P 32 F1(6)	28359656.412	-0.442<	P 4 A1(0)	28412810.623	-0.011	R 77 F1(5)	28516080.476	0.002
P 33 F2(4)	28359689.209	-0.013	Q 51 F1(6)	28412817.981	-0.002	R 77 F2(4)	28516080.476	0.002
P 33 A2(1)	28359780.517	0.035	P 4 F1(0)	28412827.541	-0.006	R 94 A2(7)	28516092.006	0.000
P 33 F2(5)	28359881.944	-0.014	Q 40 A1(0)	28412836.556	0.009	R 94 E (15)	28516092.006	0.000
P 33 E (3)	28359915.362	-0.009	P 4 E (0)	28412839.590	-0.001	R 94 F2(23)	28516092.006	0.000
P 33 F1(6)	28359960.590	0.017	Q 45 A1(2)	28412840.627	-0.035	R 70 A1(2)	28516133.528	0.020
Coincidences with R10 of N_2O (a)			Q 40 F1(1)	28412842.743	0.011	R 86 A1(6)	28516135.490	0.002
P 3 F1(0)	28414538.220	-0.007				R 86 E (13)	28516135.490	0.002
Q 35 F1(7)	28414544.247	0.041				R 86 F1(19)	28516135.490	0.002
Q 43 F1(5)	28414545.046	-0.001				R 69 F2(12)	28516214.198	-0.023
P 3 F2(0)	28414556.241	-0.012				R 70 F1(6)	28516224.553	-0.004
Q 35 E (4)	28414557.644	0.043				R 71 F1(9)	28516235.869	0.020
Q 39 F2(6)	28414564.734	-0.013				R 69 E (8)	28516236.825	-0.051
Q 43 E (3)	28414567.138	-0.013				R 67 A1(4)	28516240.568	0.015
Q 35 F2(7)	28414571.252	0.050				R 67 F1(15)	28516240.600	0.015
P 3 A2(0)	28414578.726	-0.011				R 67 F2(15)	28516240.632	0.015
Q 40 A1(1)	28414592.446	-0.029				R 67 A2(5)	28516240.664	0.014
Q 37 F1(7)	28414593.720	0.008				R 71 F2(9)	28516246.975	0.007
						R 69 F1(13)	28516254.852	-0.058
						R 81 F1(3)	28516266.540	0.001
						R 81 F2(3)	28516266.540	0.001

Note. For each laser line which has been used in the present work, we indicate the transitions of SF_6 which are in close coincidence: rovibrational assignment (branch, J_0 , C_0 , and n_0), final observed frequency in MHz (after deconvolution of the fine structure line from its hyperfine structure), and difference (obs. - calc.) frequencies in MHz. Lines which are marked with (<) are kept outside the numerical fit.

As for the eight lines which irremediably remain out of the final fit, the observed deviations are really too large (with respect to σ_d and to the experimental accuracy) to look for "accidental" reasons such as experimental or computational errors. On

the other hand, they are too small to set forth wrong rovibrational assignments (what is also completely excluded by the observed hyperfine structures). Moreover, it is striking that:

- (1) all these lines belong to the P branch, that is, are related to $(R = J + 1)$ sublevels of $(\nu_3 = 1)$;
- (2) the corresponding values of J are very limited and almost regularly spaced ($J = 31, 58-59, \text{ and } 82$);
- (3) the deviations of components of the implied multiplets (see Table III) are exactly the same, just as if these structures were simply shifted in their whole, independent of the symmetry species.

These features are illustrated on Fig. 4, where the computed energies of the $(\nu_3 = 1)$ state have been plotted versus J . The black dots indicate the manifolds for which fine structures have been observed in the present work, and the arrows point to those structures where discrepancies appear between computed and measured frequencies. Everything seems to suggest that another vibrational level actually crosses the $(R = J + 1)$ branch of ν_3 . Such a local resonance, leading to a global shift of the fine structures has already been observed in the spectrum of $\nu_1 + \nu_4$ of methane and

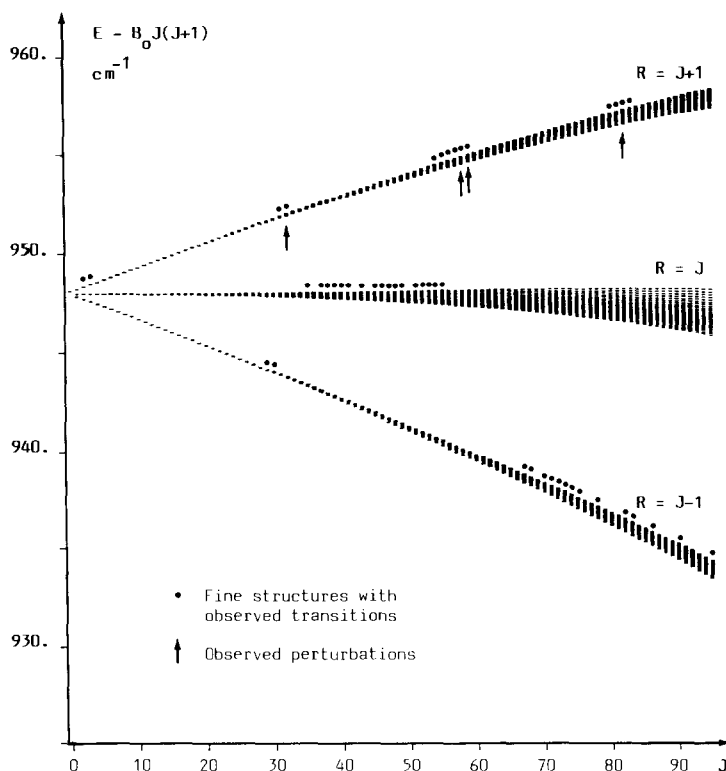


FIG. 4. Energy diagram for the $(\nu_3 = 1)$ vibrational state of SF_6 . The computed rovibrational energies, with the main rotational term $B_0 J(J + 1)$ cut out, are plotted versus J . The black dots indicate manifolds for which fine structures have been observed in the present work, and arrows point to those structures where discrepancies appear between computed and measured frequencies.

was attributed by Bobin and Guélachvili (49) to a crossing with the upper branches of the $\nu_3 + \nu_4$ level.

In the present case, we should look for a vibrational level close to ν_3 which could interact in a similar manner. The problem seems difficult to solve. Indeed, the only vibrational level which is close enough to ν_3 , and for which a real crossing with ν_3 is possible, is $\nu_4 + \nu_6$, whose center is only 13.8 cm^{-1} higher (around 961.9 cm^{-1}). Unfortunately, no pure vibrational interaction can occur between the two levels because they are of opposite parities (respectively, F_{1u} and $A_{2g} + E_g + F_{1g} + F_{2g}$), and the interaction operator would be of parity u , which is forbidden (the Hamiltonian must be A_{1g}).

But the possibility of hyperfine interactions between these two levels cannot be excluded a priori: for XY_6 octahedral molecules, there is an elementary spin operator of symmetry F_{1u} . This operator, which is noted $S^{1(u,F_{1u})}$ by Michelot (Ref. (35), p. 294), can appear in the Hamiltonian only when it is coupled with vibrational operators which are off-diagonal versus the quantum numbers ν , and of parity u ; and this is exactly what would happen in the present case. Nevertheless, although we have not yet carried out a complete calculation, we think that this attractive possibility must be dismissed for two serious reasons:

(1) the interaction operator that we can build in this way will have matrix elements depending on the hyperfine quantum numbers, and the hyperfine structures therefore should be considerably perturbed, which is not the case;

(2) the energy contribution of the implied operator will be certainly smaller than the main hyperfine terms, that is a few tenths of a MHz, whereas the observed discrepancies reach almost 2 MHz.

So, if we reject the hyperfine interactions to explain the observed perturbations, there remains only the possibility of pure vibrational ones, but involving one or several other levels of parity u . In this case, there are three possible candidates: $\nu_5 + \nu_6$, $\nu_2 + \nu_6$, and $3\nu_6$, whose centers are located, respectively, around 870.0 , 990.0 , and 1040.4 cm^{-1} . But one must notice that these levels are too far from ν_3 to allow a real crossing with ν_3 for J values lower than 100. So, in this hypothesis, the perturbations of ν_3 would not be limited to a few J values but would involve, more or less strongly, any manifold. As a consequence, the apparent localization that we observe should be simply considered as the result of the limited sampling of the present measurements.

A deeper understanding of this problem can be brought by new measurements involving a larger number of ν_3 manifolds. But these measurements must be accurate enough to detect perturbations as weak as a fraction of a MHz, that is about 10^{-5} cm^{-1} . Conventional infrared techniques are then excluded, since we require a sub-Doppler resolution. So, we have to wait for new results from saturated absorption experiments involving various isotopic species of CO_2 lasers.

Anyway, if vibrational interactions are actually responsible for the observed discrepancies, only a complete calculation involving all the implied levels can bring a satisfactory solution to the numerical problem. One will understand that, from this numerical point of view, we are not yet prepared to analyze such "polyads" of heavy spherical tops, because of the dimensions that the Hamiltonian matrices would reach even at rather low- J values. Besides, the tensor form in the $O(3)$ group, which has been used in the present work, would no longer be well adapted to the problem, and

TABLE IV—Continued

12-16-18 (continued)				CO ₂ ISOTOPE 13-16-16 BAND I							
Q87 F2(20)	28384288.487	P24	-74.424	Q77 F2(6)	28411032.540	P23	122.415	R68 F2(4)	28515130.063	P19	-23.812
F20 F2(2)	28384325.223	P24	-37.688	Q77 F1(6)	28411032.543	P23	122.418	R69 F1(11)	28515204.491	P19	50.616
F20 F1(2)	28384351.517	P24	-11.394	Q84 E(9)	28411042.873	P23	132.748	R69 F2(10)	28515282.956	P19	129.081
Q84 A1(0)	28384413.997	P24	51.086	Q84 F1(14)	28411042.873	P23	132.748				
Q84 A2(0)	28384413.997	P24	51.086	Q84 A1(5)	28411042.873	P23	132.748	R89 F2(20)	28540790.616	F18	61.235
Q84 F2(0)	28384413.997	P24	51.086	Q76 E(8)	28411047.703	P23	137.578	R89 E(13)	28540790.616	F18	61.235
Q84 F1(0)	28384413.997	P24	51.086	Q76 F1(12)	28411047.706	P23	137.581	R89 F1(21)	28540790.617	F18	61.236
F20 A1(0)	28384433.805	P24	70.894	Q76 A1(4)	28411047.710	P23	137.585				
F20 F1(1)	28384495.676	P24	132.765	Q47 A2(3)	28411051.049	P23	140.924				
				Q53 F1(8)	28411059.942	P23	149.817				
Q54 F1(5)	28410807.133	P23	-102.992	R10 E(1)	28437304.734	P22	42.086	P82 E(9)	28247354.231	R42	-32.842
Q50 F1(3)	28410815.211	P23	-94.914	R10 F2(2)	28437306.088	P22	43.440	P82 F2(14)	28247354.231	R42	-32.842
Q59 E(4)	28410832.817	P23	-77.308	R10 A2(0)	28437309.014	P22	46.366	P82 A2(4)	28247354.231	R42	-32.842
Q59 F2(7)	28410838.086	P23	-72.039	Q91 F1(0)	28437411.410	P22	148.762	P85 F2(14)	28247418.428	R42	31.355
Q59 A2(2)	28410848.384	P23	-61.741	Q91 F2(0)	28437411.410	P22	148.762	P86 F1(3)	28247424.074	R42	37.001
Q45 F1(10)	28410875.318	P23	-34.807	R27 F1(5)	28463281.087	P21	-139.578	P86 E(2)	28247424.273	R42	37.200
Q45 E(6)	28410878.122	P23	-32.003	R28 E(3)	28463545.141	P21	124.476	P86 F2(3)	28247424.472	R42	37.399
Q45 F2(9)	28410880.991	P23	-29.134	R28 F2(5)	28463545.349	P21	124.684	P84 E(6)	28247461.174	R42	74.101
Q54 A1(2)	28410906.360	P23	-29.176	R28 A2(1)	28463545.767	P21	125.102	P84 F2(10)	28247463.701	R42	76.628
Q51 F1(8)	28410952.251	P23	42.126	R27 A1(1)	28463567.716	P21	147.051	P85 E(9)	28247465.062	R42	77.989
Q53 F2(7)	28410953.503	P23	43.378	R27 F1(6)	28463569.723	P21	149.058	P84 A2(3)	28247468.842	R42	81.769
Q58 F1(7)	28410964.325	P23	54.200	R46 F1(2)	28489243.042	P20	-141.311	P80 A1(5)	28247471.712	R42	84.639
Q58 F2(7)	28410978.066	P23	67.941	R46 E(1)	28489255.946	P20	-128.407	P80 F1(16)	28247471.712	R42	84.639
Q42 A1(0)	28410987.657	P23	77.532	R46 F2(2)	28489266.600	P20	-117.753	P85 F1(15)	28247517.794	R42	130.721
Q42 F1(0)	28410987.893	P23	77.768	R47 F1(6)	28489424.409	P20	40.056				
Q42 F2(0)	28410988.128	P23	78.003	R47 F2(6)	28489450.419	P20	66.066	P72 F1(1)	28280534.064	R44	-96.751
Q42 A2(0)	28410988.364	P23	78.239					P72 E(0)	28280534.074	R44	-96.741
Q52 A2(1)	28411010.815	P23	100.690	R87 A2(0)	28515016.118	F19	-137.757	P72 F2(1)	28280534.085	R44	-96.730
Q80 E(9)	28411012.081	P23	101.956	R87 E(0)	28515016.118	F19	-137.757	P70 E(5)	28280724.484	R44	93.669
Q80 F1(13)	28411012.081	P23	101.956	R87 F2(1)	28515016.118	F19	-137.757	P70 F2(8)	28280731.571	R44	100.756
Q80 A1(4)	28411012.082	P23	101.957	R79 F1(3)	28515030.819	F19	-123.056	P70 A2(2)	28280746.605	R44	115.790
Q81 F2(6)	28411013.575	P23	103.450	R79 F2(3)	28515030.819	F19	-123.056				
Q81 F1(6)	28411013.576	P23	103.451	R66 F1(1)	28515047.162	F19	-106.713	P57 A1(4)	28313136.891	R46	-95.250
Q79 F2(6)	28411014.737	P23	104.612	R66 E(0)	28515047.201	F19	-106.674	P57 F1(14)	28313136.897	R46	-95.244
Q79 F1(6)	28411014.738	P23	104.613	R66 F2(1)	28515047.240	F19	-106.635	P57 F2(13)	28313136.904	R46	-95.237
Q82 A2(4)	28411019.212	P23	109.087	R73 F1(6)	28515066.628	F19	-87.247	P57 A2(4)	28313136.910	R46	-95.231
Q82 F2(14)	28411019.212	P23	109.087	R73 F2(6)	28515066.634	F19	-87.241	P56 F1(3)	28313273.316	R46	41.175
Q82 E(9)	28411019.213	P23	109.088	R68 F1(4)	28515084.845	F19	-69.030	P56 E(2)	28313293.917	R46	61.776
Q78 A2(4)	28411021.553	P23	111.428	R72 F2(11)	28515087.566	F19	-66.309	P56 F2(3)	28313309.803	R46	77.662
Q78 F2(13)	28411021.555	P23	111.430	R72 F1(10)	28515087.629	F19	-66.246				
Q78 E(8)	28411021.556	P23	111.431	R68 E(3)	28515107.239	F19	-46.636	P41 F2(9)	28345237.139	R48	50.726
Q51 E(5)	28411027.642	P23	117.517	R84 A2(6)	28515119.451	F19	-34.424	P41 E(6)	28345237.244	R48	50.881
Q83 F2(6)	28411028.982	P23	118.857	R84 E(12)	28515119.451	F19	-34.424	P41 F1(10)	28345237.299	R48	51.036
Q83 F1(6)	28411028.982	P23	118.857	R84 F2(19)	28515119.451	F19	-34.424	P40 E(3)	28345320.630	R48	134.217

the Laboratoire de Spectromie of Paris. The resolution is $1.2 \times 10^{-3} \text{ cm}^{-1}$ and the absolute calibration of wavenumbers (with reference to CO₂ lines) is about $0.2 \times 10^{-3} \text{ cm}^{-1}$. Unfortunately the pressure of the gas is rather high and most ν_3 lines are blended. Despite this (and the fact that many hot bands are excited at room temperature), we could identify and assign all the computed transitions, up to $J = 95$. Of course, at this resolution, almost all lines are multiplets, some Q lines covering up to 50 different transitions. The standard deviation between our computed wavenumbers and the observed ones is $1.2 \times 10^{-3} \text{ cm}^{-1}$, including all transitions, which is close to the HWHM of single nonblended lines (most lines being two or three times wider). As mentioned above, the resolution, though remarkable for this type of spectroscopy, is too weak to show evidence of the interaction between ν_3 and other vibrational levels.

To complete this section, and in order to bring to experimentalists valuable information for the development of new measurements, we give a list of calculated coincidences between SF₆ and laser lines of other isotopic species of CO₂ (Table IV). For internal consistency, all the reference frequencies of CO₂ lines have been taken from Freed *et al.* (52), where the mean accuracy is only 50 to 60 kHz. In Table IV, we give, for each isotopic species, the SF₆ rovibrational assignments followed by the computed

TABLE IV—Continued

13-16-16 (continued)				R31 F1(0)	28466380.116	R56	-52.160	P29 E(3)	28367826.810	R28	-124.854	
				R31 F2(0)	28466380.116	R56	-52.160	P29 F1(6)	28367842.205	R28	-109.459	
				R29 F2(6)	28466505.314	R56	73.038	P28 F2(6)	28367938.487	R28	-13.177	
P40 F2(5)	28345326.808	R48	140.395	R29 E(4)	28466506.730	R56	74.454	P28 F1(5)	28367938.519	R28	-13.145	
				R29 F1(7)	28466508.094	R56	75.818					
P24 E(2)	28376388.064	R50	-100.708	R30 F2(5)	28466550.526	R56	118.250	Q70 F2(2)	28398971.709	R30	-142.560	
P24 F2(4)	28376389.124	R50	-99.648	R30 F1(4)	28466552.282	R56	120.006	Q70 E(1)	28398972.207	R30	-142.062	
P24 A2(1)	28376391.287	R50	-97.485					Q70 F1(2)	28398972.707	R30	-141.562	
Q93 A1(7)	28376399.884	R50	-88.888	R51 F1(8)	28494954.259	R58	-119.420	Q81 F2(12)	28398977.472	R30	-136.797	
Q93 A2(7)	28376399.884	R50	-88.888	R50 F1(1)	28495037.918	R58	-35.761	P12 A2(0)	28398990.720	R30	-123.549	
Q93 F1(23)	28376399.884	R50	-88.888	R50 E(1)	28495038.605	R58	-35.074	P12 P2(0)	28399016.256	R30	-98.013	
Q93 F2(22)	28376399.884	R50	-88.888	R50 F2(1)	28495039.289	R58	-34.390	Q77 A1(4)	28399023.423	R30	-90.846	
				R52 A1(2)	28495116.180	R58	42.501	P12 P1(0)	28399030.794	R30	-83.475	
Q56 F2(2)	28406989.021	R52	-145.106	R52 F1(6)	28495123.857	R58	50.178	P12 A1(0)	28399042.031	R30	-72.238	
Q62 F1(5)	28406993.368	R52	-140.759	R52 E(4)	28495127.849	R58	54.170	Q90 E(7)	28399097.692	R30	-16.577	
Q56 A2(0)	28406994.243	R52	-139.884	R53 F1(5)	28495130.148	R58	56.469	Q90 F1(11)	28399098.674	R30	-15.595	
Q65 A2(3)	28407003.599	R52	-130.528	R53 F2(4)	28495130.325	R58	56.646	Q90 A1(4)	28399100.634	R30	-13.635	
Q65 F1(9)	28407014.086	R52	-120.041	R51 A1(2)	28495204.781	R58	131.102	Q84 F1(9)	28399160.082	R30	45.813	
Q82 E(8)	28407035.447	R52	-98.680					Q67 A2(5)	28399186.617	R30	72.348	
Q82 F1(12)	28407035.461	R52	-98.666					Q67 P2(15)	28399186.669	R30	72.400	
Q82 A1(4)	28407035.489	R52	-98.638					Q67 F1(15)	28399186.721	R30	72.452	
Q60 F2(4)	28407104.978	R52	-29.149					Q67 A1(4)	28399186.773	R30	72.504	
Q81 F2(7)	28407113.336	R52	-20.791					Q88 A1(2)	28399198.076	R30	83.807	
Q81 F1(8)	28407113.377	R52	-20.750					Q81 P1(12)	28399198.311	R30	84.042	
Q58 F2(3)	28407132.183	R52	-1.944					Q84 F2(9)	28399199.212	R30	84.942	
Q62 F2(5)	28407135.390	R52	1.263									
Q69 E(5)	28407135.778	R52	1.651	P87 F1(7)	28236273.461	R20	-48.299	Q79 A2(0)	28429426.241	R32	-146.732	
Q64 E(4)	28407139.377	R52	5.250	P87 F2(8)	28236273.463	R20	-48.297	Q79 E(0)	28429426.241	R32	-146.732	
Q69 F2(8)	28407141.358	R52	7.231	P90 F1(5)	28236426.578	R20	104.818	Q79 F2(1)	28429426.241	R32	-146.732	
Q69 A2(2)	28407152.284	R52	18.157	P88 F2(12)	28236433.142	R20	111.382	R 5 F1(0)	28429457.760	R32	-115.213	
Q58 E(2)	28407159.177	R52	25.050	P90 E(3)	28236433.261	R20	111.501	R 5 P2(0)	28429469.403	R32	-103.570	
Q60 E(2)	28407169.089	R52	34.962	P88 F1(11)	28236433.486	R20	111.726	R 5 E(0)	28429499.867	R32	-73.106	
Q58 F1(3)	28407186.128	R52	52.001	P90 F2(5)	28236439.946	R20	118.186	R 5 F1(1)	28429505.513	R32	-67.460	
Q80 A2(3)	28407195.248	R52	61.121					Q69 F1(0)	28429537.790	R32	-35.183	
Q80 F2(12)	28407195.306	R52	61.179	P75 F1(11)	28270126.904	R22	-143.563	P91 F2(0)	28429537.790	R32	-35.183	
Q80 E(8)	28407195.335	R52	61.208	P75 A1(3)	28270261.563	R22	-8.904	Q91 F1(1)	28429567.289	R32	94.316	
Q53 F1(12)	28407197.229	R52	63.102					Q91 F2(2)	28429567.289	R32	94.316	
Q53 E(7)	28407197.934	R52	63.807	P60 F2(6)	28303518.958	R24	-8.051					
Q53 F2(11)	28407198.640	R52	64.513	P60 F1(6)	28303558.840	R24	31.831	R46 E(3)	28488239.569	R36	-125.764	
Q64 F1(6)	28407200.059	R52	65.932	P58 E(7)	28303611.069	R24	84.060	R51 P1(0)	28488251.876	R36	-113.457	
Q79 F2(8)	28407281.279	R52	147.152	P58 F2(11)	28303611.069	R24	84.060	R51 P2(0)	28488251.876	R36	-113.457	
Q79 F1(7)	28407281.361	R52	147.234	P58 A2(3)	28303611.069	R24	84.060	R50 F1(11)	28488253.017	R36	-112.316	
				P45 F2(7)	28335961.111	R26	-127.155	R50 F2(11)	28488253.017	R36	-112.316	
Q90 A2(7)	28437004.180	R54	-112.971	P45 A2(2)	28336000.323	R26	-87.943	R46 P2(5)	28488255.466	R36	-109.867	
Q90 E(14)	28437004.180	R54	-112.971					R46 A2(1)	28488295.412	R36	-69.921	
Q90 F2(22)	28437004.180	R54	-112.971					R45 F2(9)	28488431.651	R36	66.318	
				P29 F2(5)	28367811.369	R28	-140.295	R45 E(6)	28488433.249	R36	67.916	

frequencies and detunings ($\text{SF}_6 - \text{CO}_2$) (in MHz). To be short the coincidences are given only within ± 150 MHz from the CO_2 line centers. More extended tables can also be obtained from the authors. Yet this list already shows what wonderful playground the ν_3 band of the SF_6 molecule is for saturated absorption spectroscopy!

V. CONCLUSIONS

Even though the results presented in this paper appear to represent a considerable improvement in the rovibrational analysis of the ν_3 band of SF_6 and demonstrate the power of the model which we have used in association with very-high-accuracy measurements, we have to investigate how further refinements could be made.

First, in a midterm approach of the problem, we may consider two directions of improvement:

(i) As was already mentioned in Section II, a simultaneous treatment of the rovibrational and the hyperfine problems can hardly be carried out, given the extreme complexity and variety of hyperfine structures. But a further iteration between rovibrational results and the hyperfine deconvolution procedure should be performed, leading to a somewhat better determination of both types of molecular constants.

TABLE IV—Continued

13-18 (continued)				CO ₂ ISOTOPE 14-18 BAND II			
R45 F1(10)	28488434.807	R36	69.474	P69 A1(3)	28283623.192	P42	91.930
R46 F2(4)	28488511.593	R36	146.260	P64 F1(15)	28283623.258	P42	91.996
R68 A2(0)	28516542.138	R38	-149.721	P64 E (10)	28283623.258	P42	91.996
R68 F2(2)	28516542.566	R38	-149.293	P64 A1(5)	28283623.258	P42	91.996
R68 F1(2)	28516542.993	R38	-148.866	P38 F2(7)	28348162.388	P40	-22.027
R68 A1(0)	28516543.419	R38	-148.440	P38 F1(6)	28348162.479	P40	-21.936
R84 F1(18)	28516600.497	R38	-91.362	P37 F2(0)	28348164.477	P40	-19.938
R84 F2(18)	28516600.497	R38	-91.362	P37 F1(0)	28348164.477	P40	-19.938
R87 F1(1)	28516622.179	R38	-69.680	P39 F2(7)	28348213.152	P40	28.737
R87 F2(2)	28516622.179	R38	-69.680	P39 E (4)	28348237.720	P40	53.305
R75 F1(6)	28516634.296	R38	-57.563	P39 F1(7)	28348263.593	P40	79.178
R75 F2(6)	28516634.299	R38	-57.560	Q60 E (5)	28411863.592	P38	-144.397
R73 F1(8)	28516690.174	R38	-1.685	Q60 F1(8)	28411864.355	P38	-143.634
R73 F2(7)	28516690.453	R38	-1.406	Q60 A1(3)	28411865.878	P38	-142.111
R70 F1(5)	28516719.545	R38	27.686	Q45 E (5)	28411874.660	P38	-133.329
R71 A2(3)	28516721.233	R38	29.374	Q49 F1(8)	28411898.434	P38	-109.555
R74 F2(11)	28516724.677	R38	32.818	Q52 F2(6)	28411898.573	P38	-109.416
R74 F1(11)	28516724.708	R38	32.849	Q45 F2(8)	28411899.317	P38	-108.672
R91 A2(0)	28516745.948	R38	54.089	Q47 E (5)	28411899.730	P38	-108.259
R91 E (0)	28516745.948	R38	54.089	Q59 F2(6)	28411950.558	P38	-57.431
R91 F2(1)	28516745.948	R38	54.089	Q59 F1(6)	28411952.674	P38	-55.315
R71 F2(10)	28516755.419	R38	63.560	Q51 E (4)	28411992.958	P38	-15.031
R78 A1(5)	28516773.707	R38	81.848	Q47 F2(8)	28412014.569	P38	6.580
R78 E (9)	28516773.707	R38	81.848	Q51 F2(7)	28412033.000	P38	25.011
R78 F1(14)	28516773.707	R38	81.848	Q58 A2(2)	28412040.252	P38	32.263
R71 E (6)	28516774.613	R38	82.754	Q58 F2(8)	28412043.191	P38	35.202
R70 E (3)	28516808.391	R38	116.532	Q58 E (5)	28412044.650	P38	36.661
R91 E (14)	28544263.510	R40	-36.710	Q48 F2(4)	28412076.484	P38	68.495
R91 F1(22)	28544263.510	R40	-36.710	Q48 F2(1)	28412084.931	P38	76.942
R91 F2(22)	28544263.510	R40	-36.710	Q42 E (0)	28412089.487	P38	81.498
				Q42 F1(1)	28412094.231	P38	86.242
				Q51 A2(2)	28412101.802	P38	93.813
				Q57 F2(6)	28412137.071	P38	129.082
				Q57 F1(6)	28412141.098	P38	133.109
				Q48 E (2)	28412148.455	P38	140.466
				R37 F2(2)	28474848.683	P36	-146.899
				R37 F1(1)	28474848.693	P36	-146.889
				R36 F2(5)	28474982.714	P36	-12.868
				R36 F1(4)	28474991.417	P36	-4.165
				R91 A2(5)	28537025.518	P34	-115.491
				R92 F2(8)	28537193.823	P34	52.814
				P78 F2(8)	28262874.438	P48	-117.184
				P80 F1(1)	28262907.134	P48	84.488
				P80 E (1)	28262907.136	P48	-84.486
				P80 F2(1)	28262907.139	P48	-84.483
				P76 A1(4)	28262932.734	P48	-58.888
				P76 F1(12)	28262932.736	P48	-58.886
				P76 E (8)	28262932.737	P48	-58.885
				P78 F1(7)	28262944.848	P48	-46.774
				P77 A2(2)	28262993.755	P48	2.133
				P77 F2(8)	28262994.182	P48	2.560
				P77 E (5)	28262994.396	P48	2.774
				P52 A1(2)	28320224.071	P46	-122.442
				P52 F1(6)	28320231.882	P46	-114.631
				P52 E (4)	28320235.942	P46	-110.571
				P24 E (1)	28376933.327	P44	-135.246
				P24 F2(2)	28377026.578	P44	-41.995
				P24 F1(1)	28377143.246	P44	74.673
				P24 E (0)	28377178.141	P44	109.568
				P24 F2(1)	28377195.087	P44	126.514
				Q95 F1(22)	28377198.901	P44	130.328
				Q95 E (14)	28377198.901	P44	130.328
				Q95 F2(22)	28377198.901	P44	130.328
				Q90 F1(21)	28433068.389	P42	84.211
				Q90 F2(21)	28433068.389	P42	-84.211
				Q80 A1(6)	28433190.253	P42	37.653
				Q80 E (13)	28433190.253	P42	37.653
				Q80 F1(19)	28433190.253	P42	37.653
				R46 F2(4)	28488511.593	P40	-81.972
				R48 A1(3)	28488555.853	P40	-37.712
				R48 F1(8)	28488555.868	P40	-37.697
				R48 E (5)	28488555.876	P40	-37.689
				R46 F1(4)	28488566.769	P40	-26.797
				R47 F1(4)	28488599.172	P40	5.607
				R47 F2(5)	28488600.633	P40	7.068
				R46 A1(1)	28488663.798	P40	70.233
				R94 F1(3)	28543340.278	P38	-46.331
				R94 E (2)	28543340.341	P38	-46.268
				R94 F2(3)	28543340.403	P38	-46.206

(ii) Valuable information can also be brought by additional saturated absorption measurements involving isotopic CO₂ lasers; Table IV shows that such experiments would be particularly adequate for SF₆. The accuracy of the molecular constants derived from a larger set of data would be improved, and one can even expect that the most important sixth-order contributions could be estimated.

Now, in a long-term perspective, two other directions are also to be investigated:

(i) First, as mentioned in Section III, the simultaneous fit of the ground and excited state molecular constants would be greatly improved if "forbidden" transitions were observed. Although the intensities of such lines are extremely weak in the case of SF₆,⁹ the recent progress in the sensitivity of laser spectroscopy is so important that the observation of such transitions may be expected in the future (we have recently

⁹ For instance, all eigenvectors for $J = 95$ represent rovibrational states which are pure to better than 99.6%. Then, in linear absorption spectroscopy, for example, the forbidden lines will have relative intensities less than 0.4% of the one of the allowed transitions, which is consistent with the estimation obtained by Galbraith *et al.* (65) from approximations involving clustered levels. In saturation spectroscopy, the intensity ratio of forbidden and allowed transitions will be even smaller since the power four of the dipole moment is involved in the calculation.

(4) demonstrated the possibility of recording very weak lines and crossover resonances with a good long-term frequency control).

(ii) From the vibration-rotation point of view, we have already pointed out that a global analysis of ν_3 and its interacting levels would probably remove the important discrepancies appearing for some observed lines. Such treatments of polyads of vibrational levels can be done using the formalism developed by Champion (50). Many analyses have been worked out at the Dijon Laboratory for light spherical tops; among the most recent studies, we must quote those concerning the dyads (ν_2/ν_4) of $^{12}\text{CH}_4$ (66), SiH_4 (67), and $^{12}\text{CD}_4$ (68); the dyads (ν_1/ν_3) of SiH_4 (69) and GeH_4 (70); and the pentad ($\nu_1/\nu_3/2\nu_2/2\nu_4/\nu_2 + \nu_4$) of $^{12}\text{CH}_4$ (71). All these analyses lead to standard deviations of the fitted lines close to the experimental accuracy (typically 10^{-4} cm^{-1} for FT-IR spectra). In the case of ν_3 of SF_6 , with the help of extended saturation spectroscopy data, a similar procedure can be expected to reach the kilohertz accuracy. For the moment, the numerical computation involved in such a polyad treatment can hardly be foreseen for heavy molecules, because of the dimensions of the Hamiltonian matrices and of the number of implied spectroscopic parameters. Besides, this procedure requires experimental data involving transitions to (or from) all implied vibrational levels. Presently, such data are not available for SF_6 , except for a few measurements of harmonic bands (47, 53, 54) or hot bands lines (55). Nevertheless, the increasing progress in experimental and computational techniques allow us to think that these polyad calculations will be performed within the next 10 years. We should just remember that 10 years ago, though the theoretical material had already been known for a long time, a numerical analysis with the accuracy which is achieved in the present work was hardly conceivable!

As a final conclusion, let us point out that our analysis program applies to any F_2 or F_{1u} rovibrational band of a spherical top, but is of course especially adapted to heavy molecules (with J values up to 95, presently), either tetrahedral (SiF_4 , RuO_4 , $\text{XeO}_4 \cdot \cdot \cdot$) or octahedral ones (mainly the hexafluorides: WF_6 , $\text{UF}_6 \cdot \cdot \cdot$). It has recently been used with success for the ν_3 band of the four main isotopic species of OsO_4 , with a FT-IR spectrum (56); an extension of this work is now in progress since, on one hand, new isotopic FT spectra have been recorded and, on the other hand, considerable work has also been pursued, using saturated absorption spectroscopy, for many years (1, 4, 7, 17-19). A similar program could then follow on the ν_3 band of SiF_4 , for which many close coincidences with CO_2 lines have been pointed out (72) and already assigned in a detailed analysis of this band (73).

ACKNOWLEDGMENTS

The authors thank Dr. Burton J. Krohn, of the Los Alamos National Laboratories, for friendly discussions about this work at the 1985 Columbus Symposium, and for many valuable comments about the manuscript.

RECEIVED: February 18, 1986

REFERENCES

1. CH. J. BORDÉ, in "Revue du Cethedec-Ondes et Signal," NS83-1, pp. 1-118, 1983.
2. H. BRUNET AND M. PEREZ, *J. Mol. Spectrosc.* **29**, 472 (1969).
3. W. G. HARTER, *Phys. Rev. A* **24**, 192 (1981).

4. CH. J. BORDÉ, J. BORDÉ, CH. BRÉANT, CH. CHARDONNET, A. VAN LERBERGHE, AND CH. SALOMON, in "Laser Spectroscopy VII" (T. W. Hänsch and Y. R. Shen, Eds.), pp. 108–114, Springer-Verlag, New York/Berlin, 1985.
5. CH. J. BORDÉ, M. OUHAYOUN, AND J. BORDÉ, *J. Mol. Spectrosc.* **73**, 344 (1978).
6. M. OUHAYOUN AND CH. J. BORDÉ, *Metrologia* **13**, 149 (1977).
7. CH. J. BORDÉ, M. OUHAYOUN, A. VAN LERBERGHE, CH. SALOMON, S. AVRILLIER, C. D. CANTRELL, AND J. BORDÉ, in "Laser Spectroscopy IV" (H. Walther and K. W. Rothe, Eds.), p. 142, Springer-Verlag, New York/Berlin, 1979.
8. CH. SALOMON, CH. BRÉANT, A. VAN LERBERGHE, G. CAMY, AND CH. J. BORDÉ, *Appl. Phys. B* **29**, 153–155 (1982).
9. A. VAN LERBERGHE, S. AVRILLIER, CH. J. BORDÉ, AND C. D. CANTRELL, *J. Opt. Soc. Amer.* **68**, 624 (1978).
10. A. VAN LERBERGHE, S. AVRILLIER, AND CH. J. BORDÉ, *IEEE J. Quantum Electron.* **14**, 481 (1978).
11. J. BORDÉ AND CH. J. BORDÉ, *Chem. Phys.* **71**, 417–441 (1982).
12. J. BORDÉ AND CH. J. BORDÉ, *Chem. Phys.* **84**, 159 (1984).
13. CH. FREED AND A. JAVAN, *Appl. Phys. Lett.* **17**, 53 (1970).
14. F. R. PETERSEN, D. G. McDONALD, J. D. CUPP, AND B. L. DANIELSON, in "Laser Spectroscopy" (R. G. Brewer and A. Mooradian, Eds.), pp. 555–569, Plenum, New York, 1974.
15. F. R. PETERSEN, E. C. BEATY, AND C. R. POLLOCK, *J. Mol. Spectrosc.* **102**, 112 (1983).
16. S. AVRILLIER, J. M. RAIMOND, CH. J. BORDÉ, D. BASSI, AND G. SCOLES, *Opt. Commun.* **39**, 311–315 (1981).
17. A. CLAIRON, A. VAN LERBERGHE, CH. SALOMON, M. OUHAYOUN, AND CH. J. BORDÉ, *Opt. Commun.* **35**, 368–372 (1980).
18. A. CLAIRON, A. VAN LERBERGHE, CH. BRÉANT, CH. SALOMON, G. CAMY, AND CH. J. BORDÉ, *J. Phys. Coll. (Paris)* **42**, C8–127 (1981).
19. CH. CHARDONNET, A. VAN LERBERGHE, AND CH. J. BORDÉ, *Opt. Commun.* **58**, 333–337 (1986) and "Communication to 9th Colloquium on High Resolution Molecular Spectroscopy," Riccione, Italy, 1985.
20. A. CLAIRON, B. DAHMANI, A. FILIMON, AND J. RUTMAN, *IEEE Trans. Instr. Measur.* **34**, 265–268 (1985).
21. J. BORDÉ, CH. J. BORDÉ, CH. SALOMON, A. VAN LERBERGHE, M. OUHAYOUN, AND C. D. CANTRELL, *Phys. Rev. Lett.* **45**, 14 (1980).
22. CH. J. BORDÉ, in "Advances in Laser Spectroscopy, NATO ASI Series," (T. Arrechi, F. Strumia, and H. Walther, Eds.), Plenum, New York, 1983.
23. J. C. HILICO, H. BERGER, AND M. LOËTE, *Canad. J. Phys.* **54**, 1702–1711 (1973).
24. W. B. PERSON AND B. J. KROHN, *J. Mol. Spectrosc.* **98**, 229–257 (1983).
25. E. PASCAUD, *J. Phys. (Paris)* **37**, 1287 (1976).
26. M. LOËTE, Thesis, University of Dijon, France, 1984; *Canad. J. Phys.* **61**, 1242–1259 (1983).
27. K. FOX, *Opt. Commun.* **19**, 397 (1976).
28. K. FOX AND W. B. PERSON, *J. Chem. Phys.* **64**, 5218 (1976).
29. K. KIM, R. S. MCDOWELL, AND W. T. KING, *J. Chem. Phys.* **73**, 36 (1980).
30. J. BORDÉ AND CH. J. BORDÉ, *J. Mol. Spectrosc.* **78**, 353 (1979).
31. J. BORDÉ, *J. Phys. Lett. (Paris)* **12**, L175 (1978).
32. W. G. HARTER, C. W. PATTERSON, AND DA PAIXAO, *Rev. Mod. Phys.* **50**, 37 (1978).
33. F. MICHELOT, *Mol. Phys.* **45**, 949–970 and 971–1001 (1982); *J. Mol. Spectrosc.* **106**, 77–109 and 160–190 (1984); *Canad. J. Phys.* **62**, 148–157 (1984).
34. J. MORET-BAILLY, *Cah. Phys.* **15**, 237–316 (1961).
35. F. MICHELOT, Thesis, University of Dijon, France, 1980.
36. F. MICHELOT, J. MORET-BAILLY, AND K. FOX, *J. Chem. Phys.* **60**, 2610–2616 (1974).
37. J. MORET-BAILLY, L. GAUTIER, AND J. MONTAGUTELLI, *J. Mol. Spectrosc.* **15**, 355–377 (1965).
38. B. J. KROHN, unpublished results.
39. K. T. HECHT, *J. Mol. Spectrosc.* **5**, 355 (1960).
40. A. G. ROBIETTE, D. L. GRAY, AND F. W. BIRSS, *Mol. Phys.* **32**, 1591–1607 (1976).
41. B. BOBIN AND K. FOX, *J. Phys. (Paris)* **34**, 571–582 (1973).
42. J. P. ALDRIDGE, H. FILIP, H. FLICKER, R. F. HOLLAND, R. S. MCDOWELL, N. G. NERESON, AND K. FOX, *J. Mol. Spectrosc.* **58**, 165–168 (1975).

43. R. S. MCDOWELL, H. W. GALBRAITH, B. J. KROHN, C. D. CANTRELL, AND E. D. HINKLEY, *Opt. Commun.*, **17**, 178–183 (1976).
44. M. LOËTE, A. CLAIRON, A. FRICHET, R. S. MCDOWELL, H. G. GALBRAITH, J. C. HILICO, J. MORET-BAILLY, AND L. HENRY, *Compt. Rend. Acad. Sci. (Paris)* **285B**, 175–178 (1977).
45. R. S. MCDOWELL, H. W. GALBRAITH, C. D. CANTRELL, N. G. NERESON, AND E. D. HINKLEY, *J. Mol. Spectrosc.* **68**, 288–298 (1977).
46. VI. G. TYUTEREV, J. P. CHAMPION, G. PIERRE, AND V. I. PEREVALOV, *J. Mol. Spectrosc.* **105**, 113–138 (1984).
47. C. W. PATTERSON, B. J. KROHN, AND A. S. PINE, *J. Mol. Spectrosc.* **88**, 133–166 (1981).
48. H. BERGER AND A. ABOUMAJD, *J. Phys. Lett. (Paris)* **42**, L55–L57 (1981).
49. B. BOBIN AND G. GUELACHVILI, *J. Phys. (Paris)* **39**, 33–42 (1978).
50. J.-P. CHAMPION, *Canad. J. Phys.* **55**, 1802–1828 (1977).
51. L. HENRY AND A. VALENTIN, private communication, 1984.
52. CH. FREED, L. C. BRADLEY, AND R. G. O'DONNELL, *IEEE J. Quant. Electron.* **16**, 1195–1206 (1980).
53. A. S. PINE AND A. G. ROBIETTE, *J. Mol. Spectrosc.* **80**, 388–402 (1980).
54. C. W. PATTERSON, F. HERLEMONT, M. AZIZI, AND J. LEMAIRE, *J. Mol. Spectrosc.* **108**, 34–41 (1984).
55. M. DUBBS, D. HARRADINE, E. SCHWEITZER, J. I. STEINFELD, AND C. W. PATTERSON, *J. Chem. Phys.* **77**, 3824–3839 (1982).
56. B. BOBIN, A. VALENTIN, AND L. HENRY, *J. Mol. Spectrosc.*, to be published. "Communication to the 40th Molecular Spectroscopy Symposium," Columbus, Ohio, June 17–22, 1985.
57. J. S. GRIFFITH, "The Irreducible Tensor Method for Molecular Symmetry Groups," Prentice-Hall, Englewood Cliffs, N.J., 1962.
58. A. J. DORNEY AND J. K. G. WATSON, *J. Mol. Spectrosc.* **42**, 135–148 (1972).
59. C. D. CANTRELL AND H. W. GALBRAITH, *J. Mol. Spectrosc.* **58**, 158–164 (1975).
60. B. J. KROHN, private communication, 1986.
61. J. MORET-BAILLY, *J. Mol. Spectrosc.* **15**, 344–354 (1965).
62. B. J. KROHN AND J. K. G. WATSON, "Communications to the Molecular Spectroscopy Symposium," Columbus, Ohio, Paper ME-8 (1981) and Paper WE-7 (1983).
63. A. ABOUMAJD, H. BERGER, AND R. SAINT-LOUP, *J. Mol. Spectrosc.* **78**, 486–492 (1979).
64. J. P. ALDRIDGE, E. G. BROCK, H. FILIP, H. FLICKER, K. FOX, H. W. GALBRAITH, R. F. HOLLAND, K. C. KIM, B. J. KROHN, D. W. MAGNUSON, W. B. MAIER II, R. S. MCDOWELL, C. W. PATTERSON, W. B. PERSON, D. F. SMITH, AND G. K. WERNER, *J. Chem. Phys.* **83**, 34–48 (1985).
65. H. G. GALBRAITH, C. W. PATTERSON, B. J. KROHN, AND W. G. HARTER, *J. Mol. Spectrosc.* **73**, 475–493 (1978).
66. J. P. CHAMPION AND G. PIERRE, *J. Mol. Spectrosc.* **79**, 255–280 (1980).
67. G. PIERRE, A. VALENTIN, AND L. HENRY, *Canad. J. Phys.* **64**, 341–350 (1986).
68. M. LOËTE, J. C. HILICO, A. VALENTIN, J. CHAZELAS, AND L. HENRY, *J. Mol. Spectrosc.* **99**, 63–86 (1983).
69. G. PIERRE, J. P. CHAMPION, D. N. KOZLOV, AND V. V. SMIRNOV, *J. Phys. (Orsay)* **43**, 1429–1436 (1982).
70. P. LEPAGE, J. P. CHAMPION, AND A. G. ROBIETTE, *J. Mol. Spectrosc.* **89**, 440–448 (1981).
71. G. POUSSIGUE, E. PASCAUD, J. P. CHAMPION, AND G. PIERRE, *J. Mol. Spectrosc.* **93**, 351–380 (1982).
72. R. S. MCDOWELL, C. W. PATTERSON, N. G. NERESON, F. R. PETERSEN, AND J. S. WELLS, *Opt. Lett.* **6**, 422–424 and 647 (1981).
73. C. W. PATTERSON, R. S. MCDOWELL, N. G. NERESON, B. J. KROHN, J. S. WELLS, AND F. R. PETERSEN, *J. Mol. Spectrosc.* **91**, 416–423 (1982).